OMICS International

OMICS International through its Open Access Initiative is committed to make genuine and reliable contributions to the scientific community. OMICS International journals have over **3 million** readers and the fame and success of the same can be attributed to the strong editorial board which contains over **30000** eminent personalities that ensure a rapid, quality and quick review process. OMICS International signed an agreement with more than **1000** International Societies to make healthcare information Open Access.

Contact us at: contact.omics@omicsonline.org

OMICS Journals are welcoming Submissions

OMICS International welcomes submissions that are original and technically so as to serve both the developing world and developed countries in the best possible way. OMICS Journals are poised in excellence by publishing high quality research. OMICS International follows an Editorial Manager® System peer review process and boasts of a strong and active editorial board.

Editors and reviewers are experts in their field and provide anonymous, unbiased and detailed reviews of all submissions. The journal gives the options of multiple language translations for all the articles and all archived articles are available in HTML, XML, PDF and audio formats. Also, all the published articles are archived in repositories and indexing services like DOAJ, CAS, Google Scholar, Scientific Commons, Index Copernicus, EBSCO, HINARI and GALE.

For more details please visit our website:
http://omicsonline.org/Submitmanuscript.php

Chemical Sciences Journal
Open Access, Peer-reviewed
2150-3494

Synthesis and Applications of Nanoparticles of Titanium Dioxide and Zinc Oxide

Majeed A. Shaheed and Falah H. Hussein

Chemistry Department, Faculty of Science, Babylon University, Hilla, Iraq

Correspondence should be addressed to Falah H. Hussein; abohasan_hilla@yahoo.com

The work summary

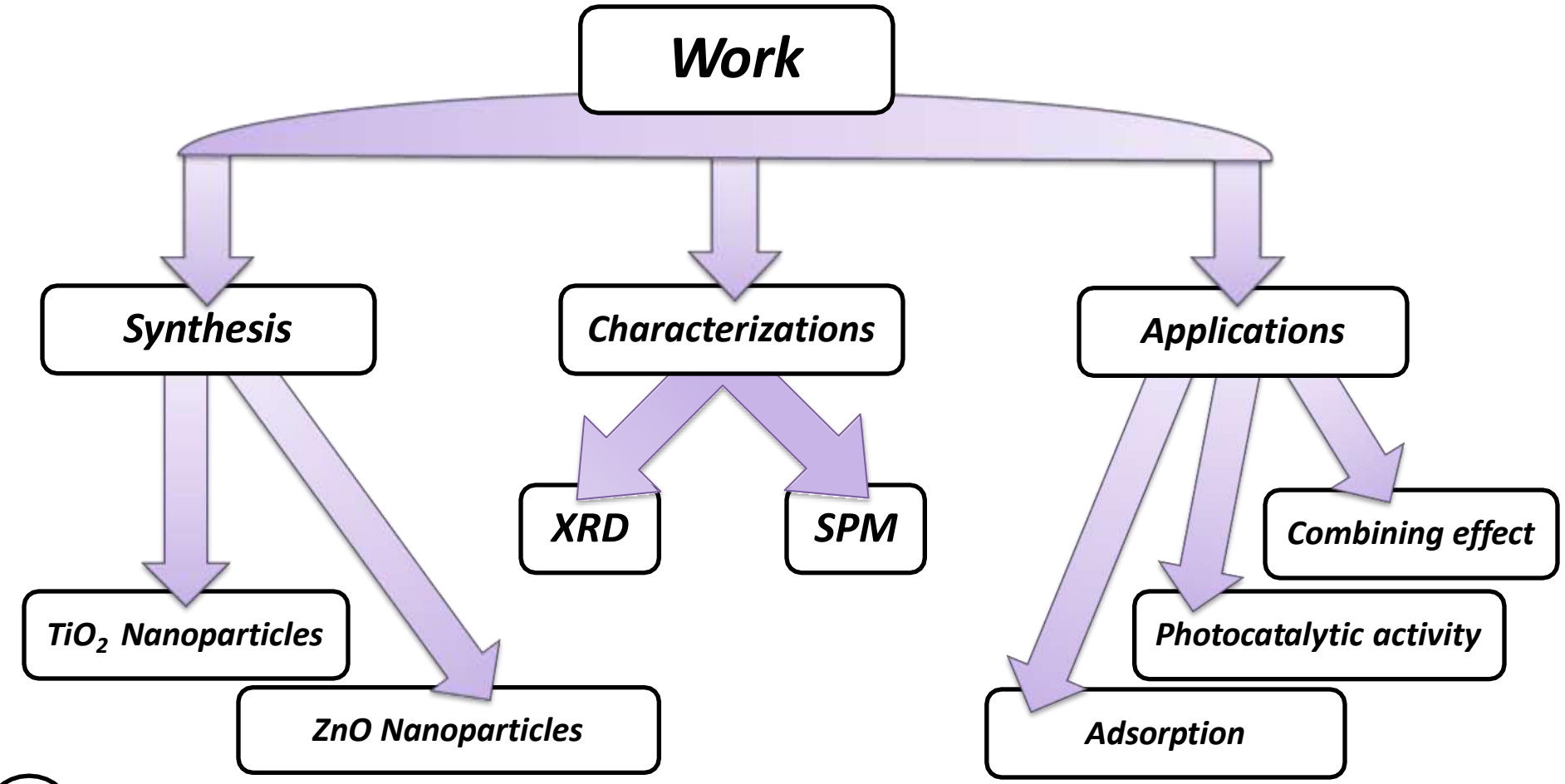

Experimental devices

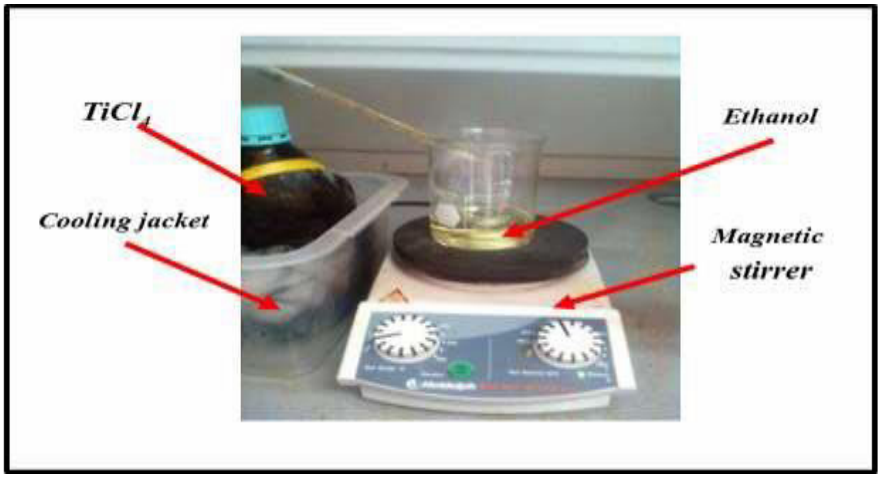

Figure 1: Sol gel Synthesis of TiO_2 nanoparticles

Figure 2: Scanning probe microscopic analysis (SPM)

Figure 3: Shaker device

Figure 4: Water bath shaker device

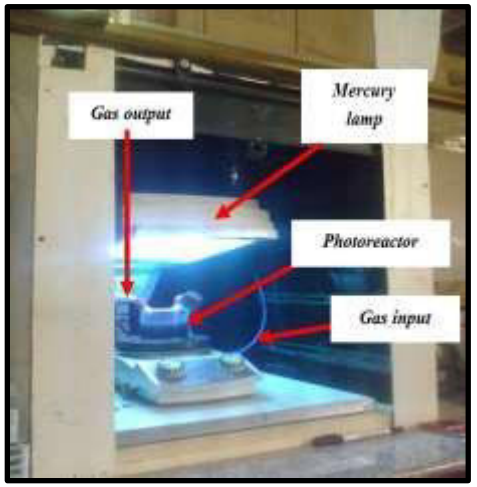

Figure 5: Photoreactor system

First: Synthesis

Synthesis of TiO_2 nanostructures by sol-gel method

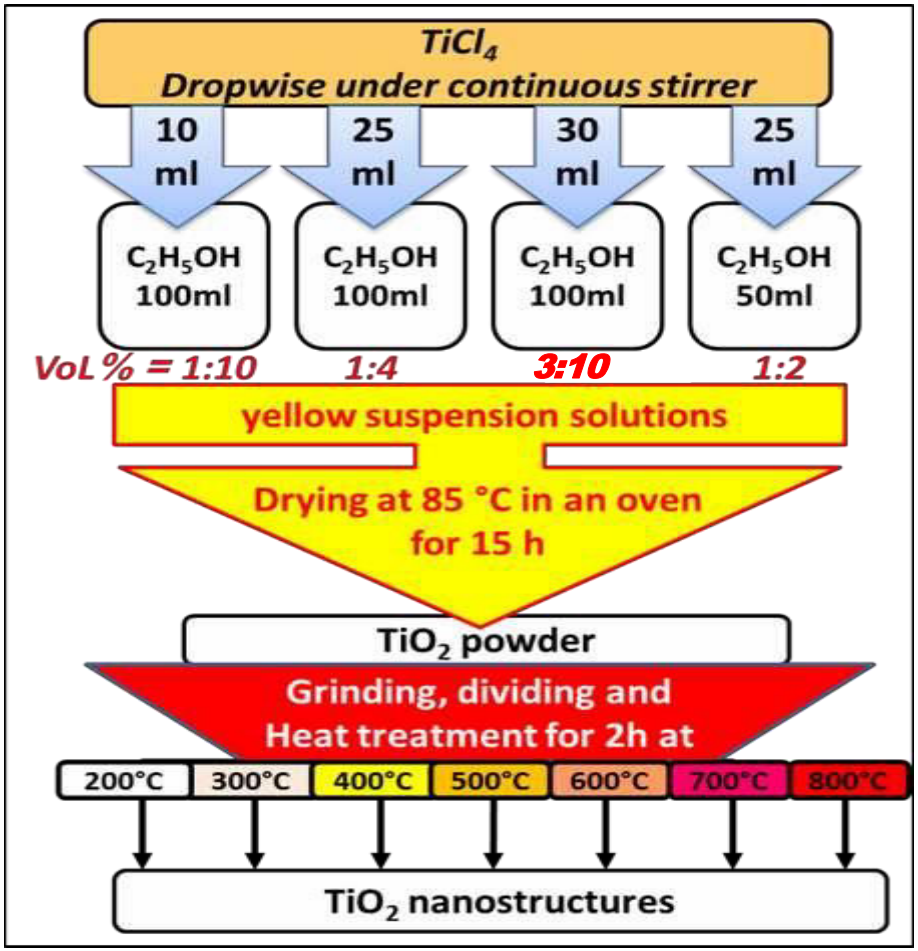

Figure 6: Detailed schematic representation for experimental procedure.

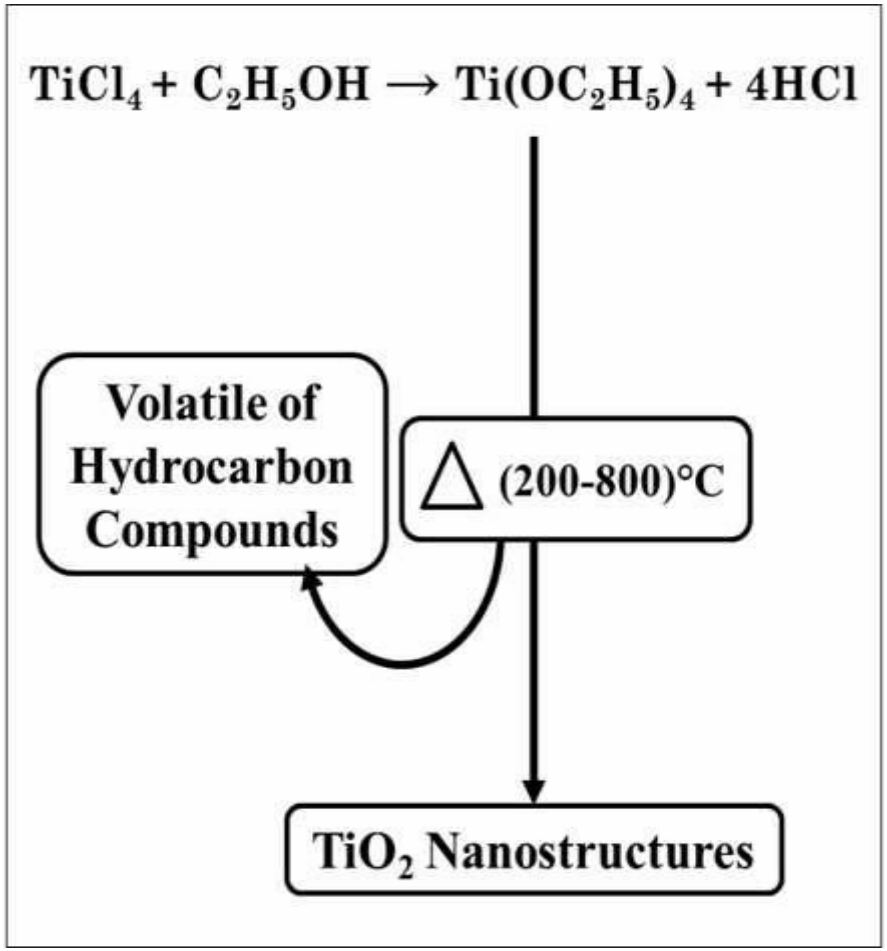

Figure 7: Schematic diagram for experimental procedure.

Other route to Synthesis of TiO_2 nanoparticles by sol gel.

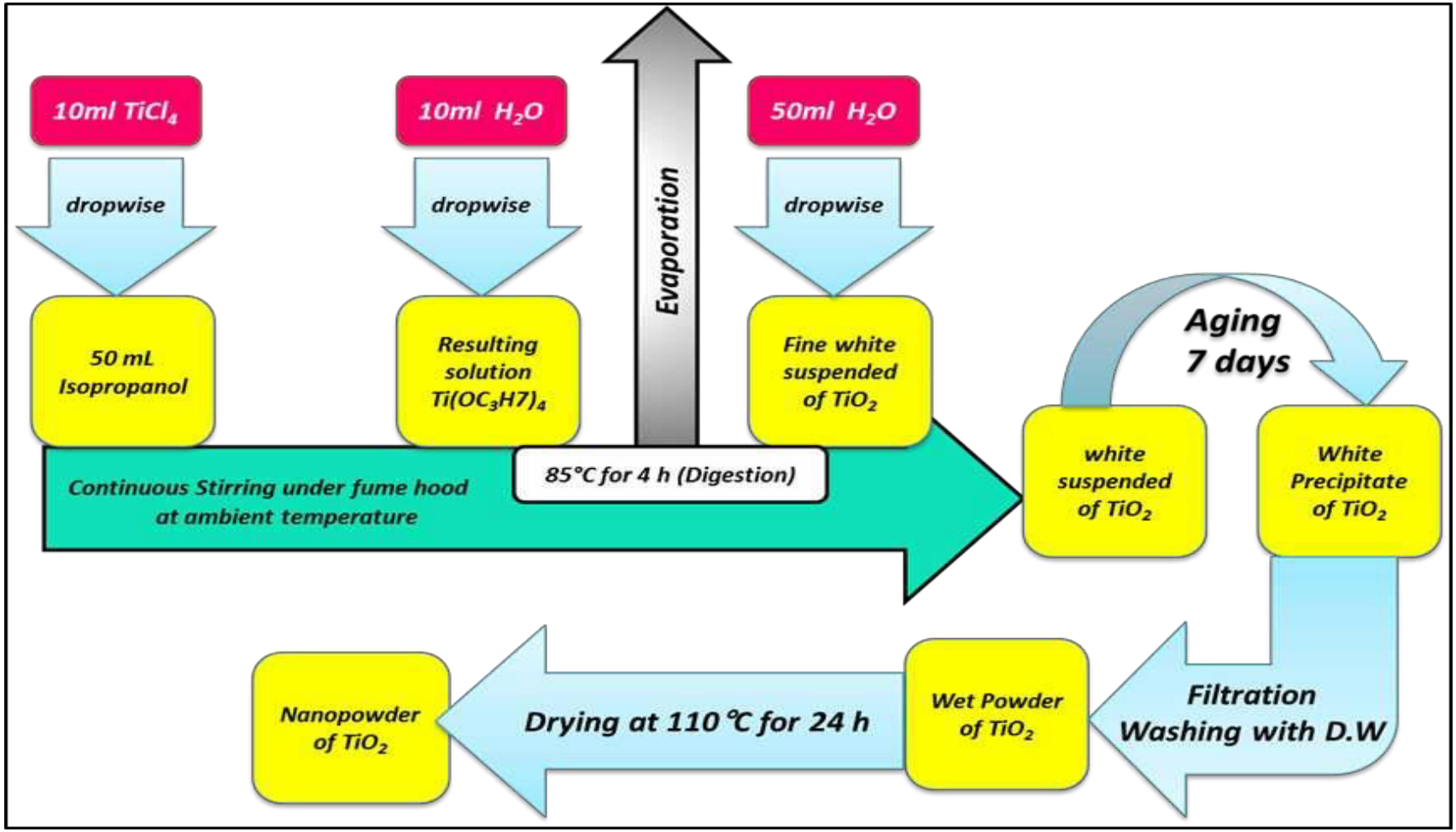

Figure 8: Schematic diagram of experimental procedure for preparation of TiO_2-NPs.

Synthesis of ZnO nanoparticles in the first route

$$ZnSO_4.7H_2O + 2NaOH \longrightarrow Zn(OH)_2 + 7H_2O + Na_2SO_4$$

$$Zn(OH)_2 + 2H_2O \longrightarrow [Zn(OH)_4]^{2-} + 2H^+ \rightarrow 3H_2O + ZnO$$

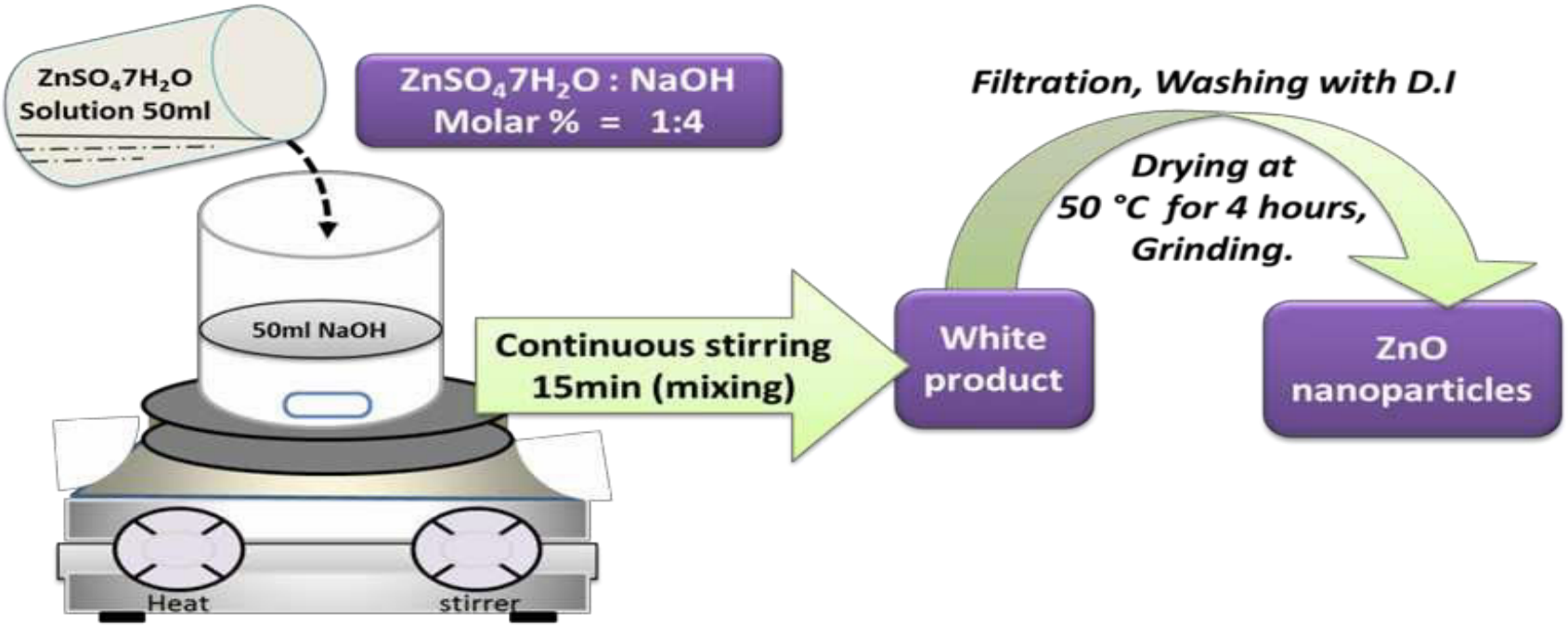

Figure 9: Schematic diagram of experimental procedure for preparation of ZnO-NPs by using the first direct precipitation method.

Synthesis of ZnO nanoparticles in the second routes

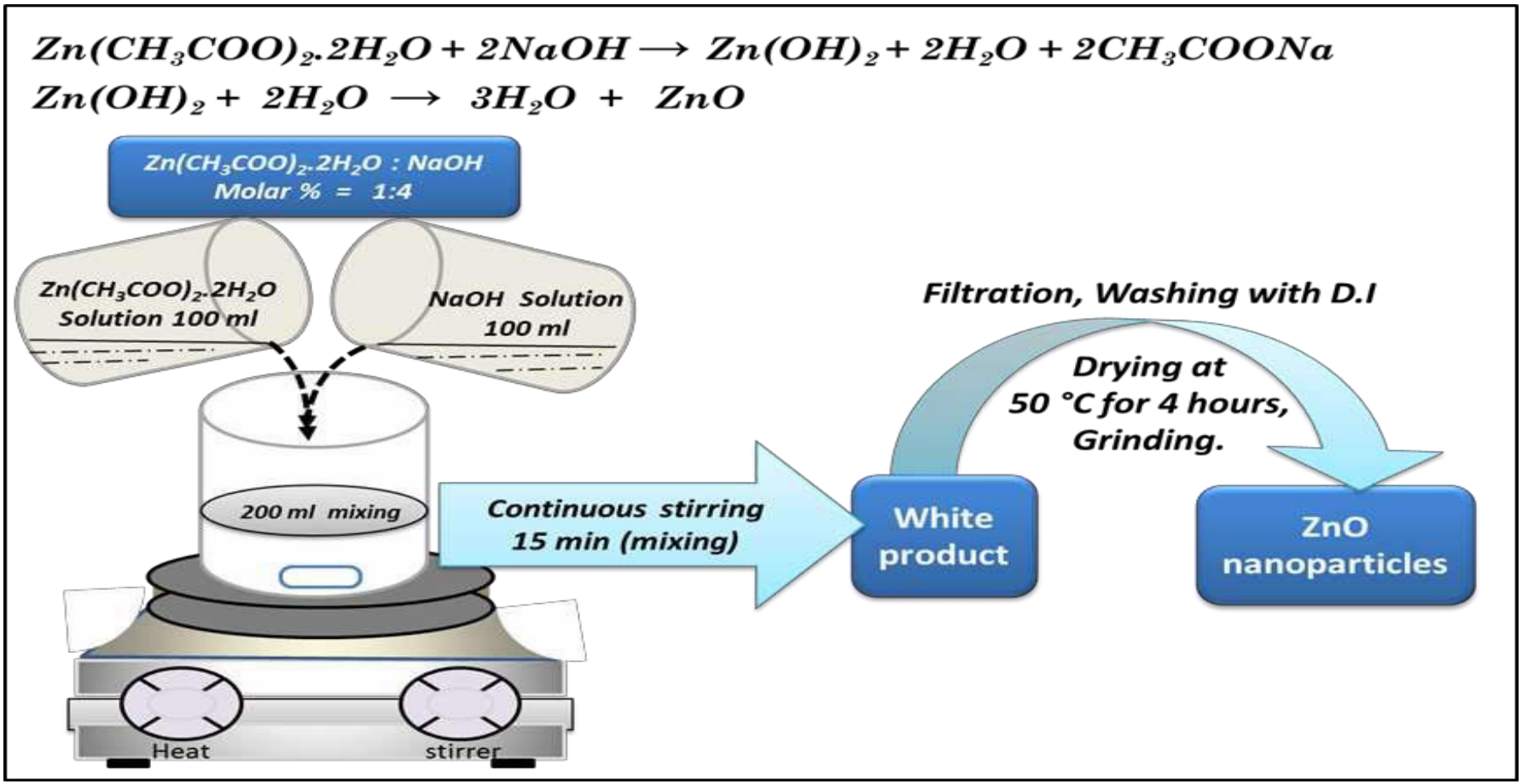

Figure 10: Schematic diagram of experimental procedure for preparation of ZnO-NPs by using the second direct precipitation method.

Second : Characterizations

1-XRD
2-SPM

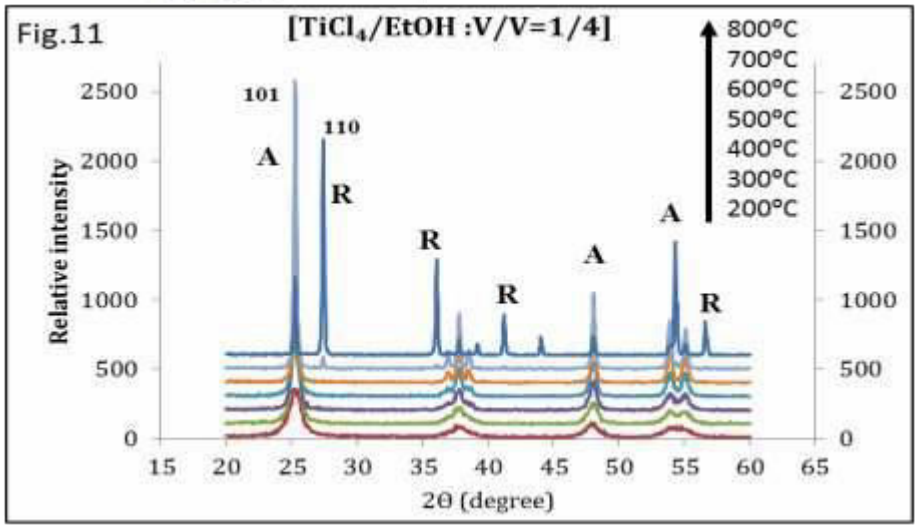

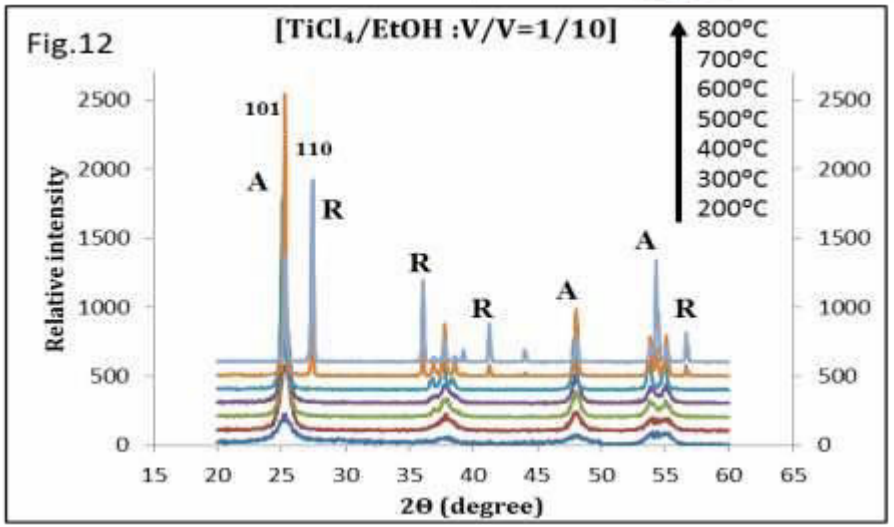

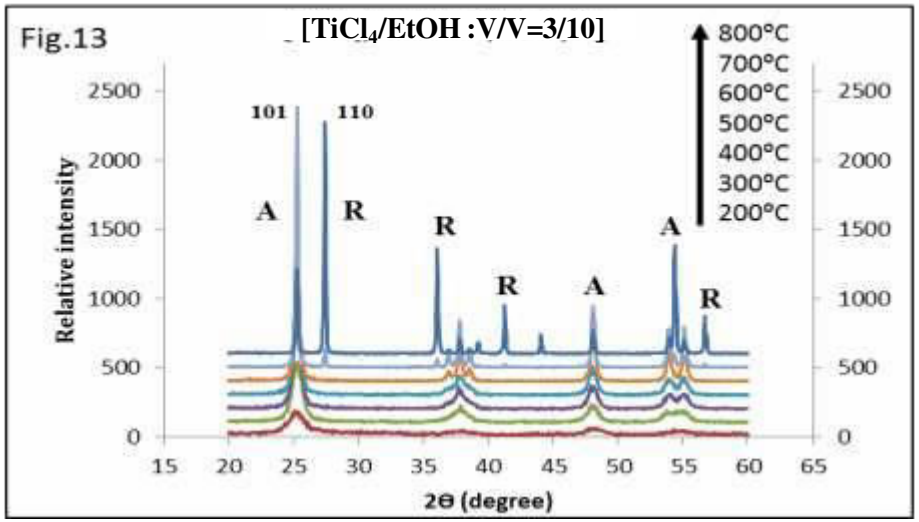

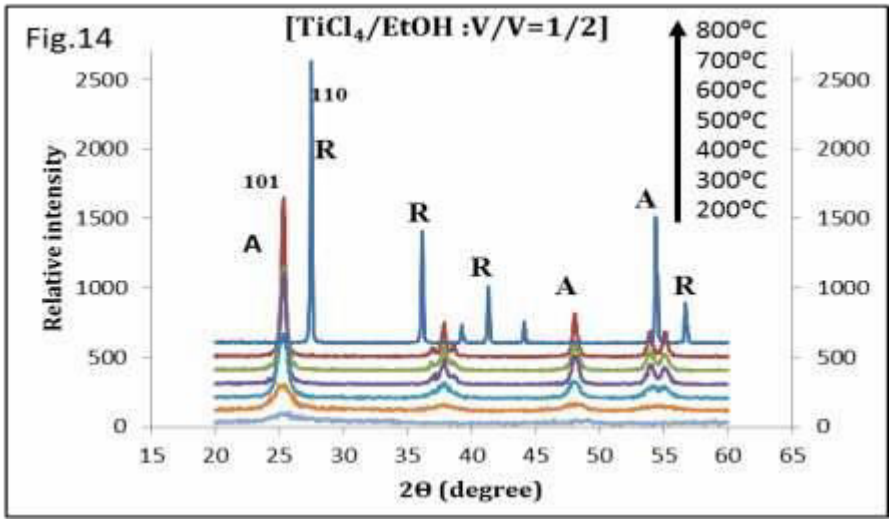

Figures 11 to 14: XRD pattern of the synthesized TiO_2-NPs with calcination temperatures between 200°C-800°C for 2 hours. A: Anatase, R: Rrutile. [V/V(TiCl4:EtOH)=1:10, 1:4, 1:3 and 1:2].

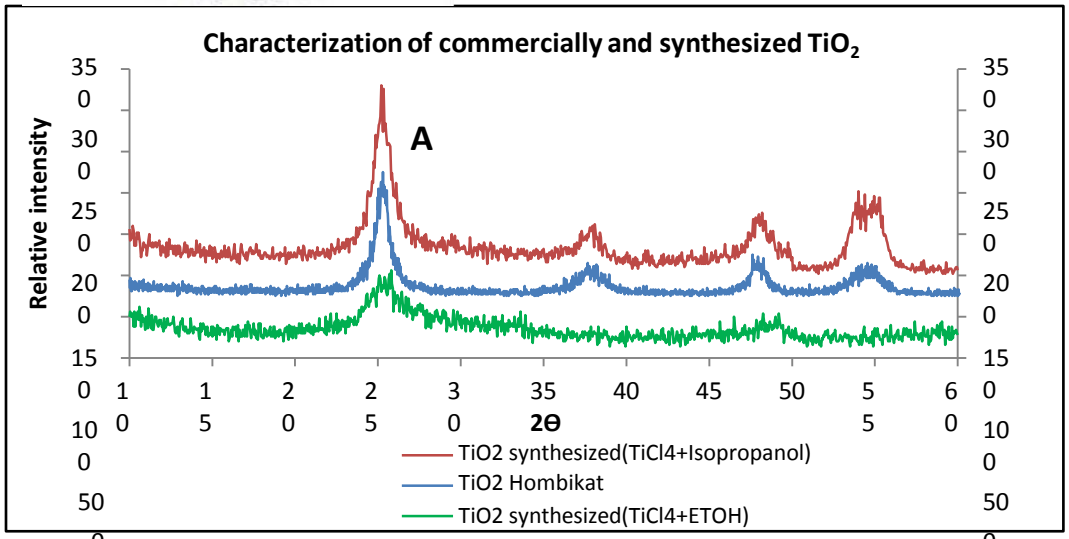

Figure 15: XRD patterns for the optimum TiO_2-NPs produced from both sol gel method with reference TiO_2 (Hombikat UV100).

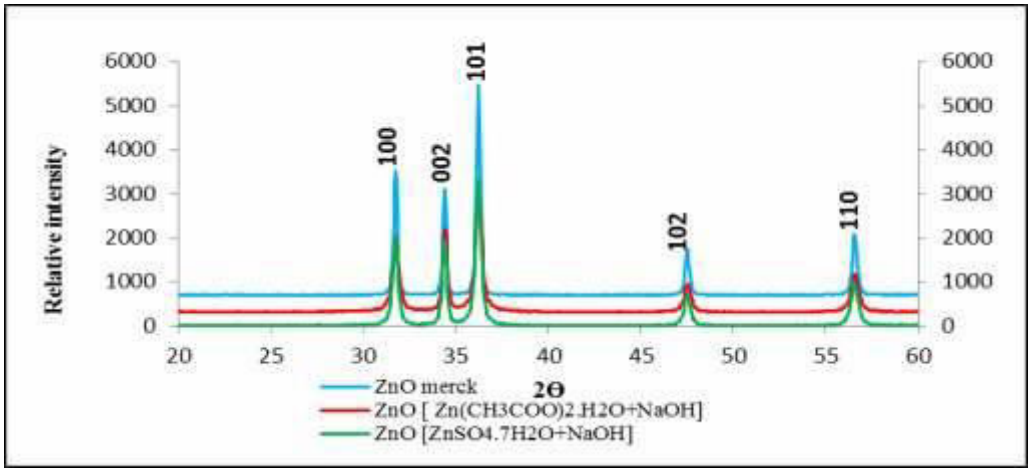

Figure 16: The comparison of XRD patterns of the ZnO-NPs resulted by the precipitation method in two different routes with the reference ZnO (Merck).

SPM	Volumetric percentage of additives ($TiCl_4$/EtOH)			
	1/10	1/4	1/3	1/2
Annealing temp =200°C	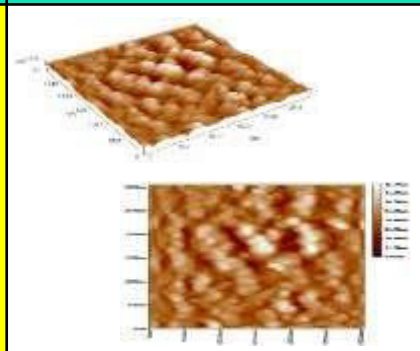	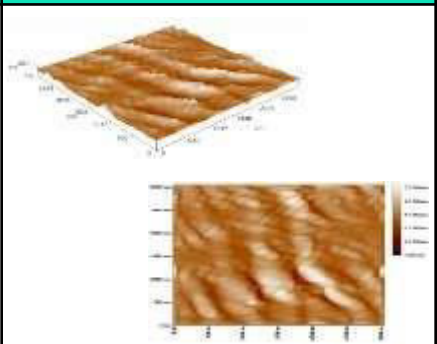	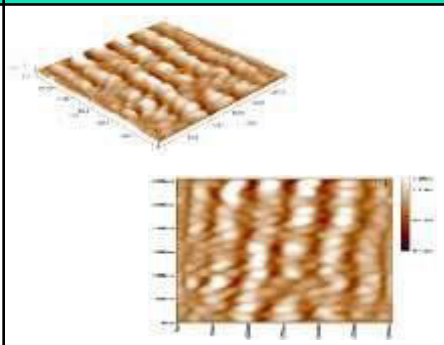	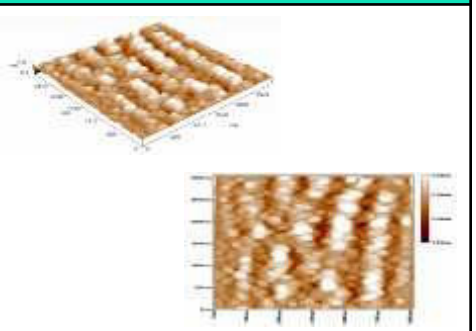
C.S (nm)	8.48	9.97	7.68	6.23
P.S (nm)	64.73	123.54	164.66	123.54
Annealing temp =800 °C	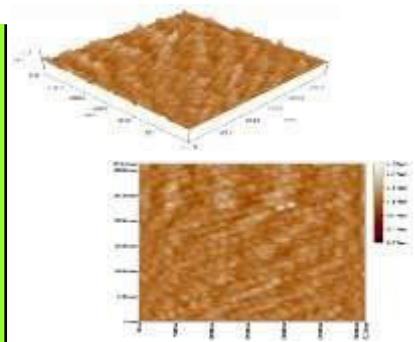	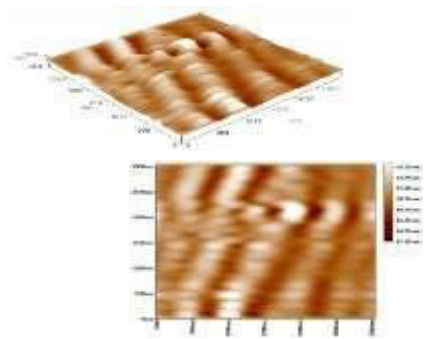	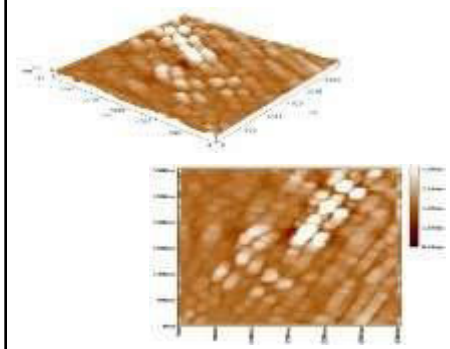	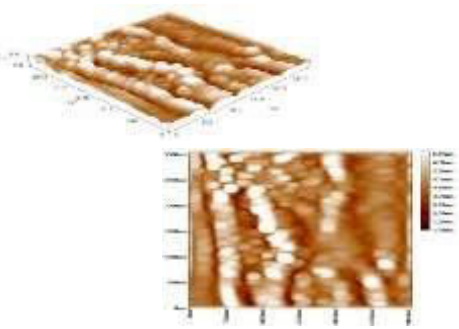
C.S (nm)	65.24	7.68	56.45	56.52
P.S (nm)	98.32	164.66	127.48	137.36

SPM	Types of semiconductor			
	TiO_2 (Hombikat UV 100)	TiO_2 prepared from ($TiCl_4$+Isopropanol+H_2O)	ZnO (merck)	ZnO prepared from ($ZnSO_4.7H_2O$+NaOH)
	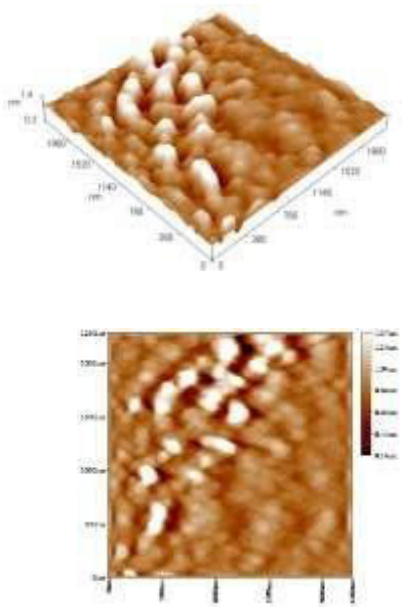	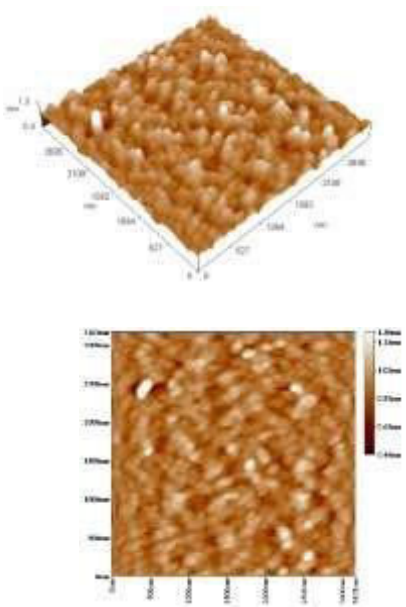	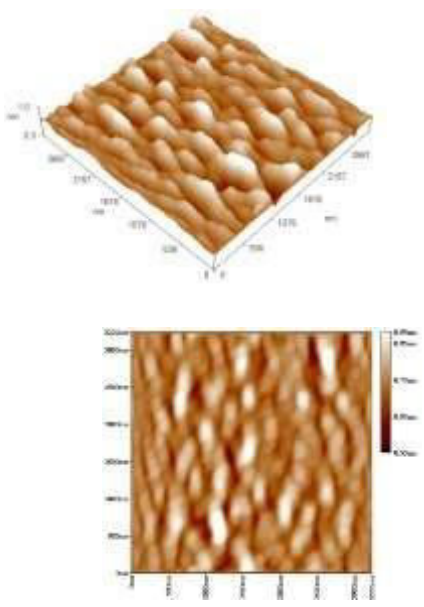	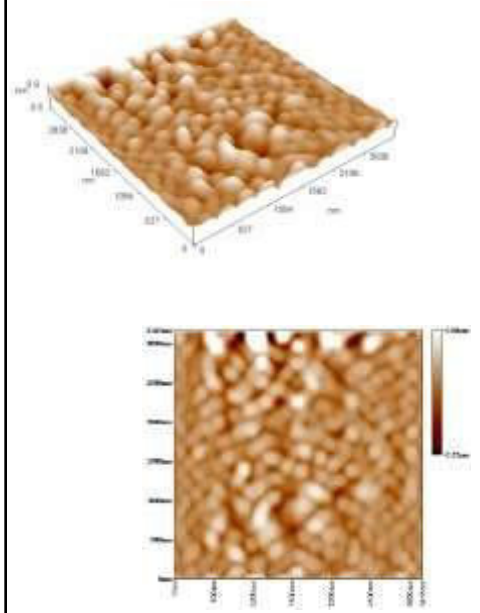
C.S (nm)	11.91	14.58	52.26	123.57
P.S (nm)	84.89	98.08	154.2	137.44

Figures 26 to 29: SPM images of the synthesized TiO_2-NPs and ZnO-NPs using second sol gel and direct precipitation method compared with references.

Table 1: Comparison between average crystallite size and particle size calculated according to XRD and SPM techniques for the prepared TiO_2-NPs in the first sol gel method

No. of TiO_2-NPs	V/V($TiCl_4$:EtOH)	Calcination temperature /°C	Average crystal size /nm	Average particle size/nm
1	1:2	800	56.52	137.36
2	1:4	800	7.68	164.66
3	1:10	800	65.24	98.32
4	1:10	500	19.02	
5	1:10	700	46.17	
6	1:3	800	56.45	127.48
7	1:3	600	62.41	
8	1:4	500	32.73	
9	1:2	400	16.11	
10	1:3	700	42.67	
11	1:2	700	70.02	
12	1:4	700	43.14	
13	1:4	600	151.40	
14	1:2	600	24.78	
15	1:10	300	12.90	
16	1:10	200	8.48	64.73
17	1:2	500	27.93	
18	1:3	400	15.94	
19	1:10	600	164.76	
20	1:3	500	24.13	
21	1:2	300	6.38	
22	1:3	200	7.68	164.66
23	1:4	200	9.97	123.54
24	1:4	300	14.47	
25	1:10	400	19.00	
26	1:3	300	12.01	
27	1:4	400	27.03	
28	1:2	200	6.23	123.54

Third : Applications

1-Adsorption
2-Photocatalytic Activity
3-Combining Effect

1-Adsorption

Calibration curve of dye in different absorption positions

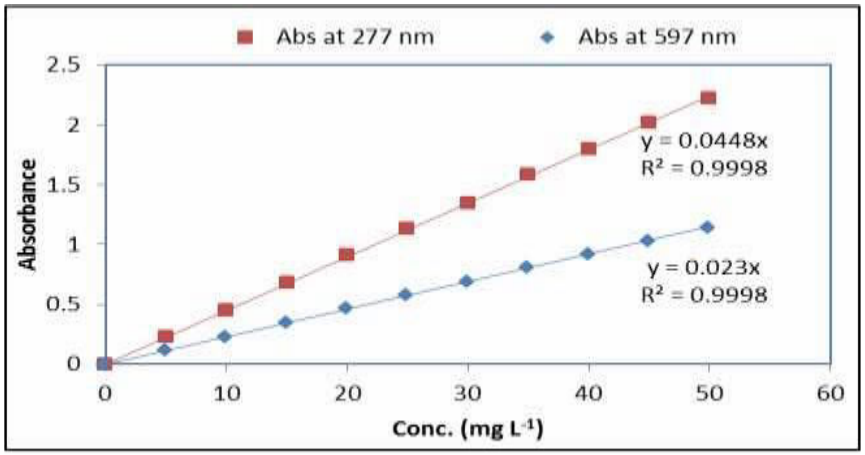

Figure 31:Calibration curve at different concentrations of 277 and 597 nm for RB 5.

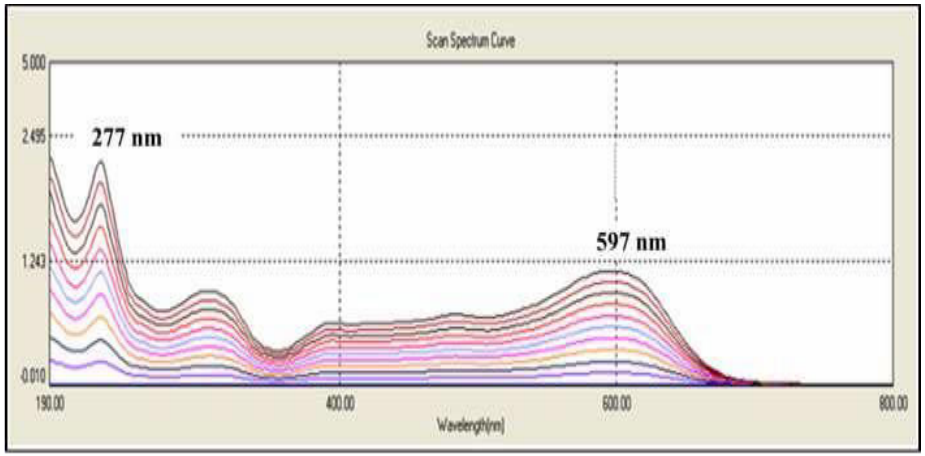

Figure 32:UV-Vis spectra of different concentrations of RB 5.

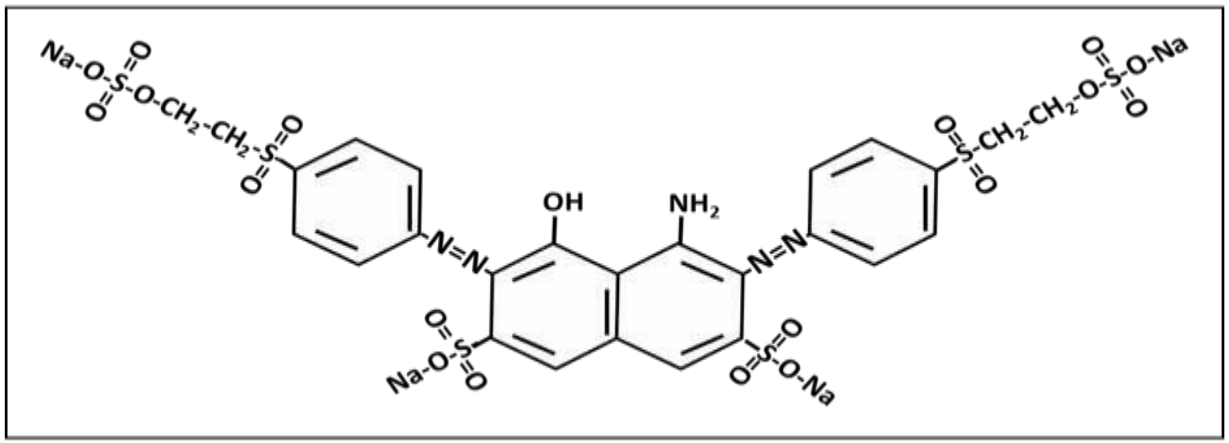

Figure 33:Chemical Structure of RB 5

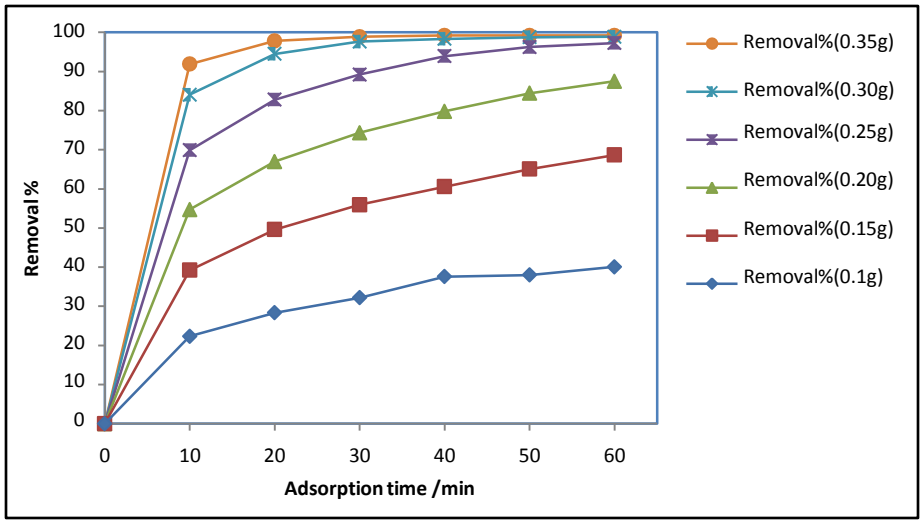

Figure 38: Effect of dose on removal percentage of RB 5.

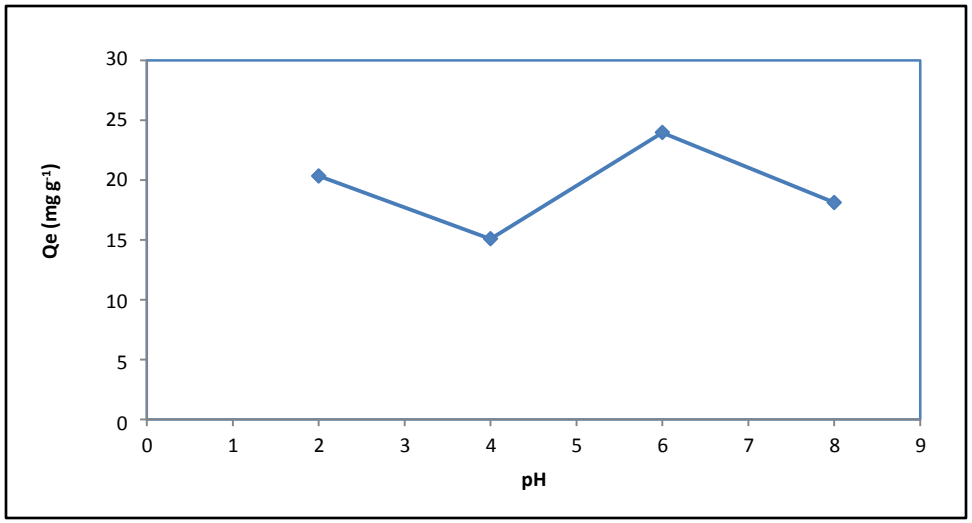

Figure 39: Effect of pH on adsorption of RB 5 solution.

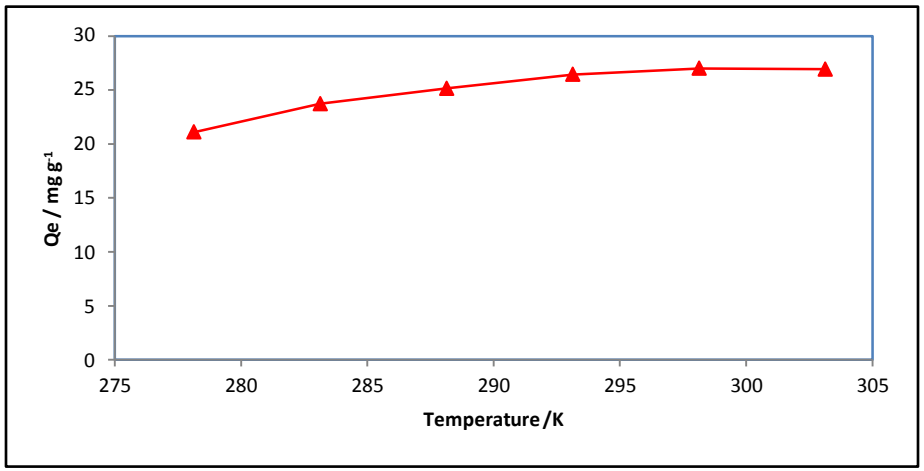

Figure 40: Effect of temperature on adsorption of RB 5 solution.

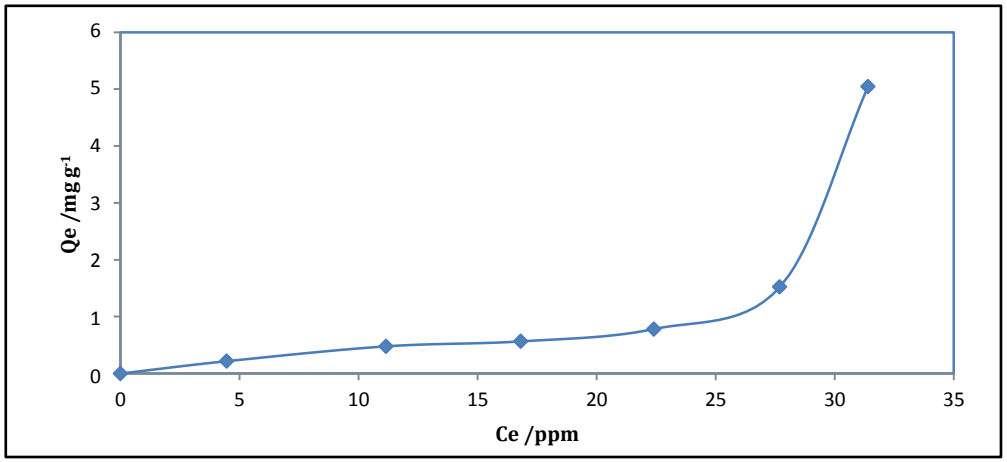

Figure 41: Adsorption isotherm of RB 5 dye in presence of TiO_2-NPs.

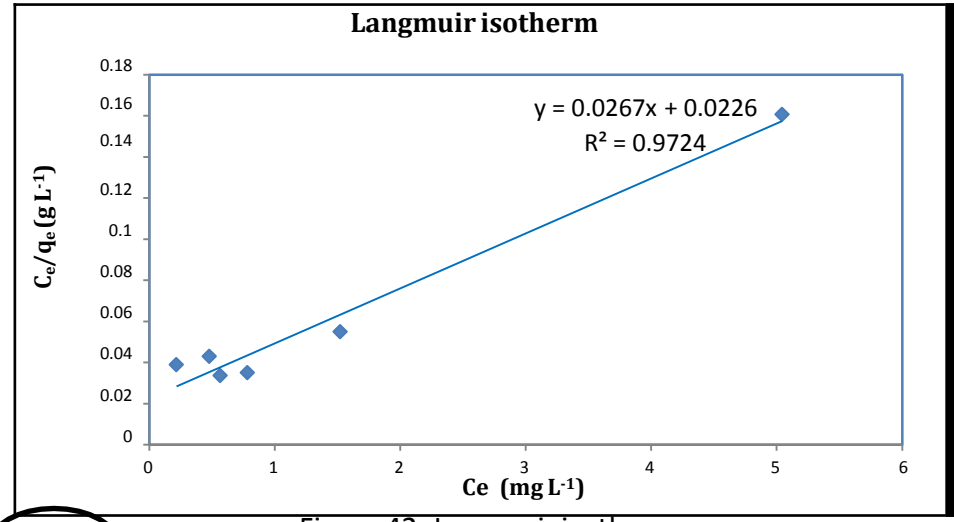

Figure 42: Langmuir isotherm.

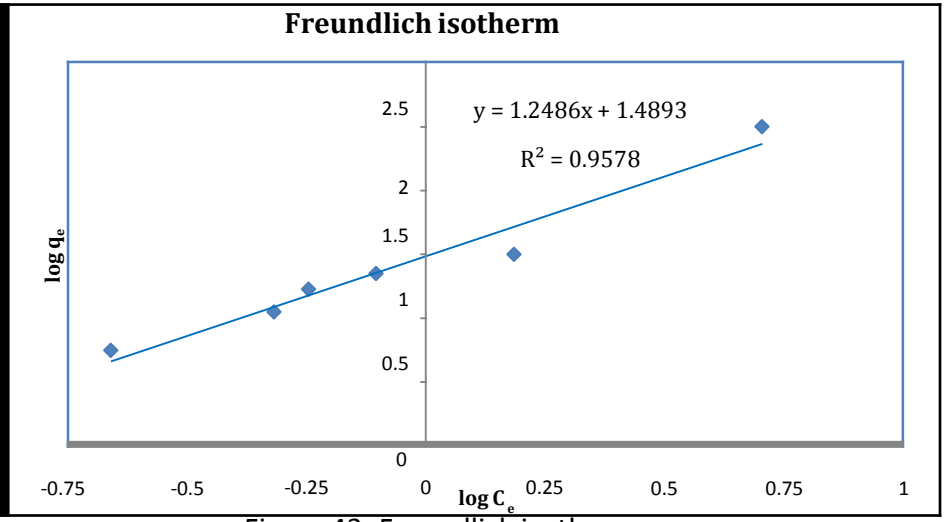

Figure 43: Freundlich isotherm.

Table 2: Adsorption constants of Langmuir and Freundlich.

Isotherm parameters for RB 5 adsorption on TiO_2-NPs		
Isotherm	**Parameters**	**Values**
Langmuir	Q_L(mg/g)	37.453
	K_L(L/mg)	1.1810
	R^2	0.9724
Frendlich	K_F	2.2190
	n	0.8009
	R^2	0.9578

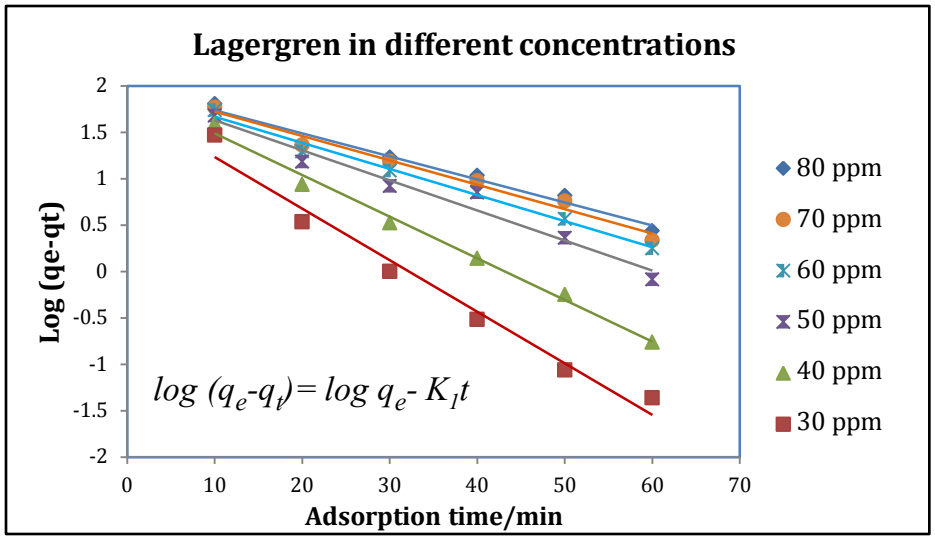

Figure 44: Pseudo first-order kinetic model.

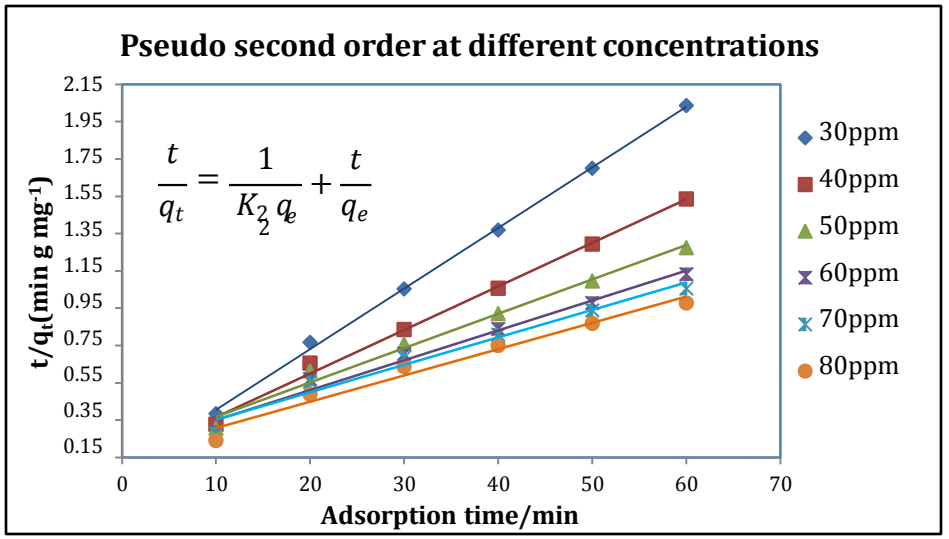

Figure 45: Pseudo second-order kinetic model.

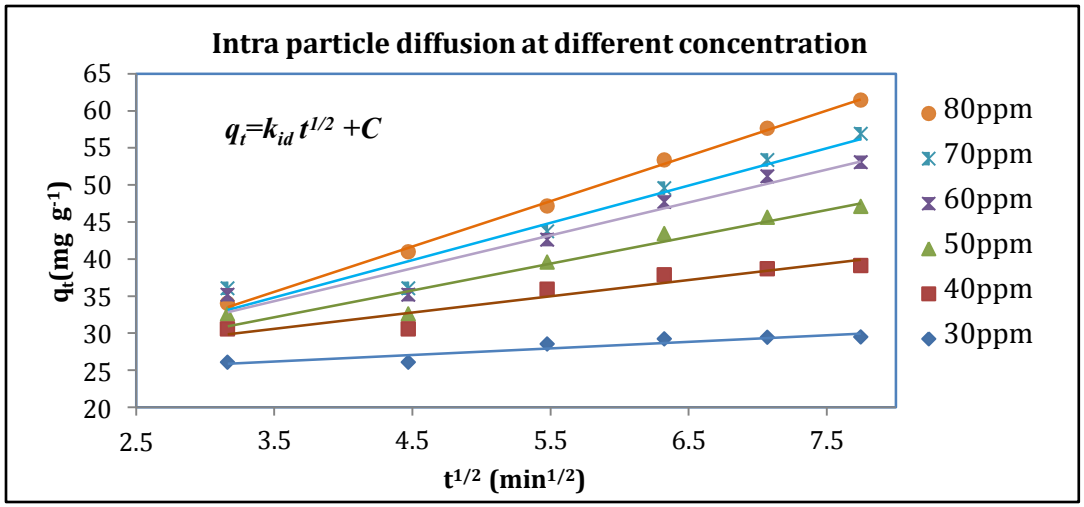

Figure 46: Intra particle diffusion model.

Table 3: Adsorption parameters for RB 5 adsorption on TiO_2-NPs.

C_o (ppm)	Pseudo first order model				
	q_e, exp (mg/g)	q_e, cal (mg/g)	K_1 min-1	R^2	S.D %
30	16.8695	0.5828	0.0240	0.9754	7.529
40	22.4347	0.6609	0.0260	0.9918	10.020
50	27.3788	0.6704	0.0280	0.9642	12.233
60	31.3292	0.6679	0.0320	0.9888	14.001
70	33.7639	0.9855	0.0440	0.9784	15.087
80	36.6708	0.6855	0.0550	0.9724	16.391
C_o (ppm)	Pseudo second order model				
	q_e, exp (mg/g)	q_e, cal (mg/g)	K_2 g/mg min	R^2	S.D %
30	16.8695	30.7692	0.0132	0.9989	6.729
40	22.4347	42.7350	0.0041	0.9951	9.181
50	27.3788	54.3478	0.0019	0.9863	11.356
60	31.3292	62.5000	0.0013	0.9792	13.119
70	33.7639	68.0272	0.0011	0.9704	14.199
80	36.6708	70.9219	0.0012	0.9720	15.535
C_o (ppm)	Intra particle diffusion model				
	q_e, exp (mg/g)	C (mg/g)	K_{id} g/mg $min^{1/2}$	R^2	S.D %
30	16.8695	23.0690	0.8879	0.8629	6.933
40	22.4348	22.9300	2.1929	0.8962	9.576
50	27.3789	19.5110	3.6157	0.9317	11.926
60	31.3292	18.8080	4.4369	0.9362	13.742
70	33.7639	17.2540	5.0252	0.9379	14.871
80	36.6708	14.1950	6.1106	0.9979	16.227

Adsorption Thermodynamics

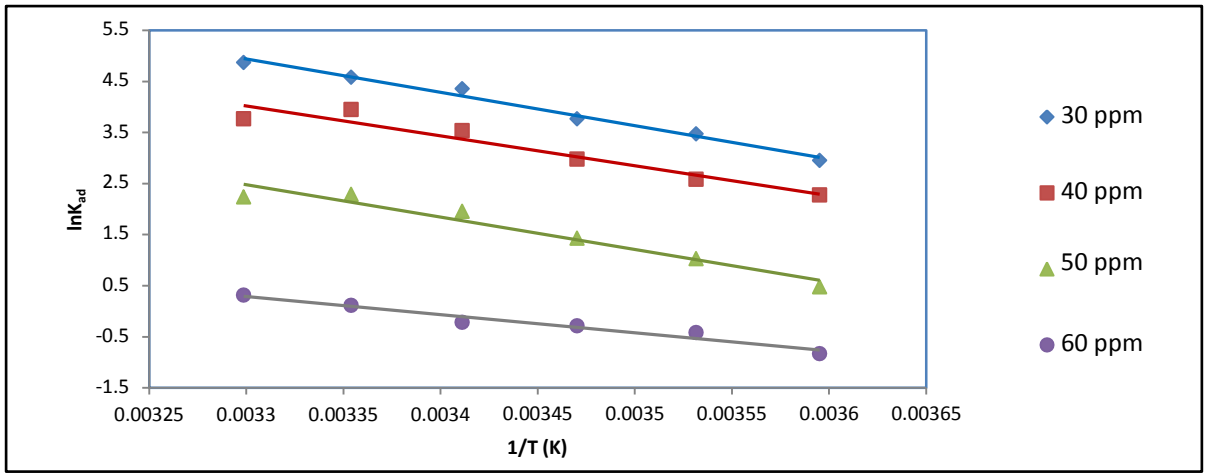

Figure 47: The plot of ln kad versus 1/T for the determination of thermodynamic parameters.

Table 4: Thermodynamic parameters at different temperatures and concentrations.

Adsorbent	ΔG°/ k J mol^{-1}							ΔH° / k J mol^{-1}	ΔS° /k J mol^{-1}K^{-1} x10-3
	C/ppm	5 °C	10 °C	15 °C	20 °C	25 °C	30 °C		
TiO_2-NPs	30	-6.815	-8.166	-9.009	-10.610	-11.346	-12.264	54.248	26.509
	40	-5.254	-6.075	-7.122	-8.614	-9.778	-9.478	48.651	23.368
	50	-1.102	-2.418	-3.427	-4.759	-5.663	-5.634	52.714	23.441
	60	1.918	0.987	0.690	0.528	-0.282	-0.794	29.633	12.073

2-Photocatalytic Activity

Dark and irradiation reaction

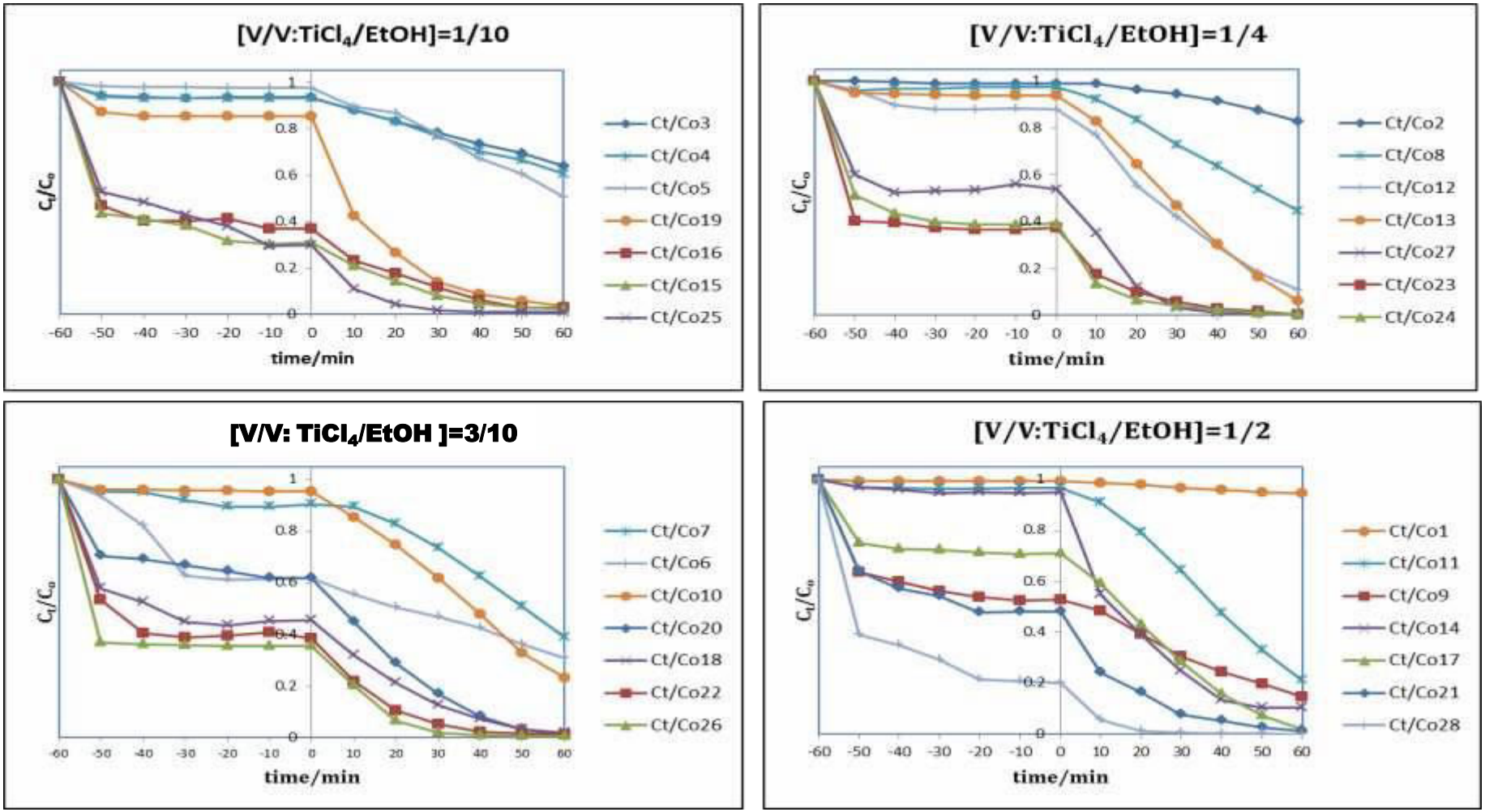

Figures 48 to 51: Dark reaction and irradiation at different types of the prepared TiO_2-NPs. [V/V($TiCl_4$:EtOH)=1:10, 1:4, 1:3 and 1:2].

Dark and irradiation reaction

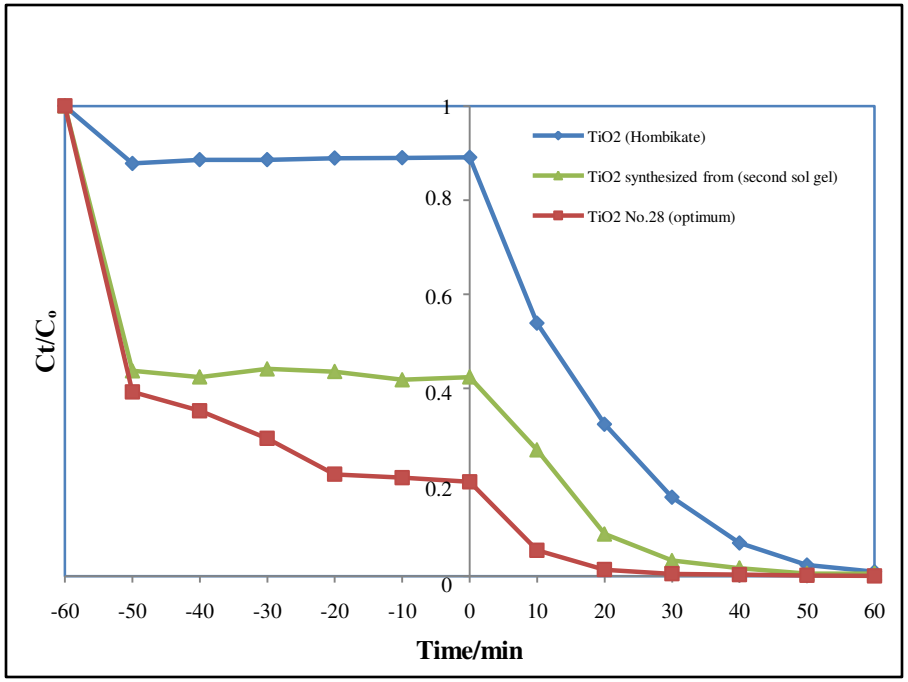

Figure 52: Dark reaction and irradiation at the optimum two types of the prepared TiO_2-NPs with TiO_2 (Hombikat UV100).

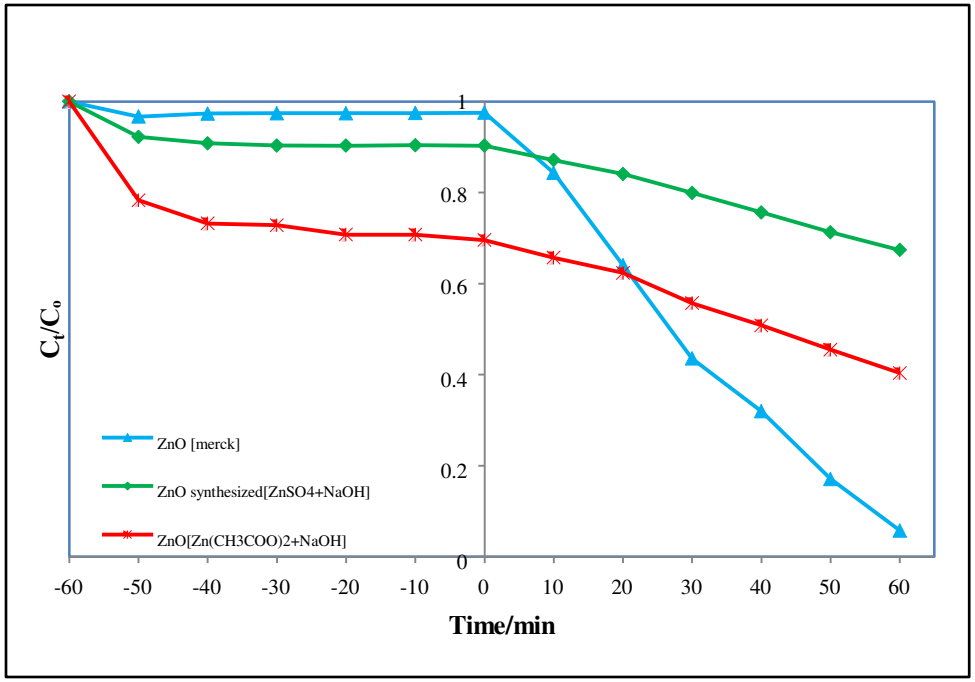

Figure 53: Dark reaction and irradiation at the different two types of the prepared ZnO-NPs with ZnO (Merck).

Variations of decolorization efficiencies

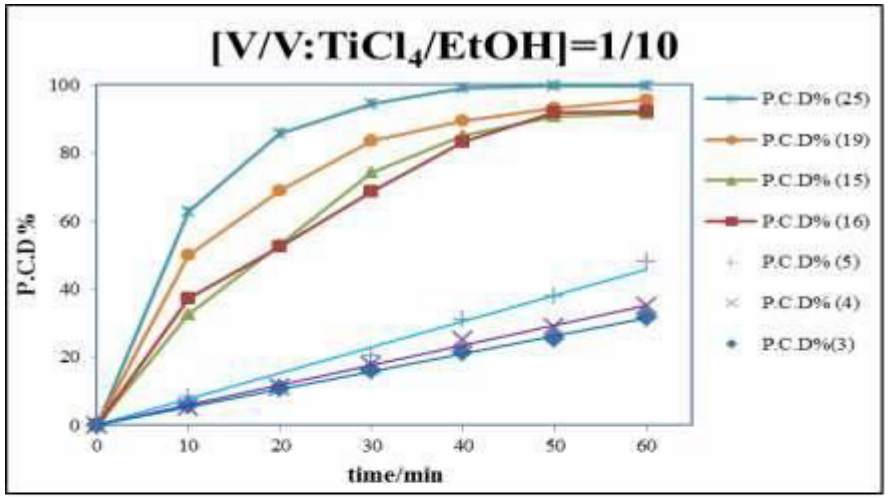

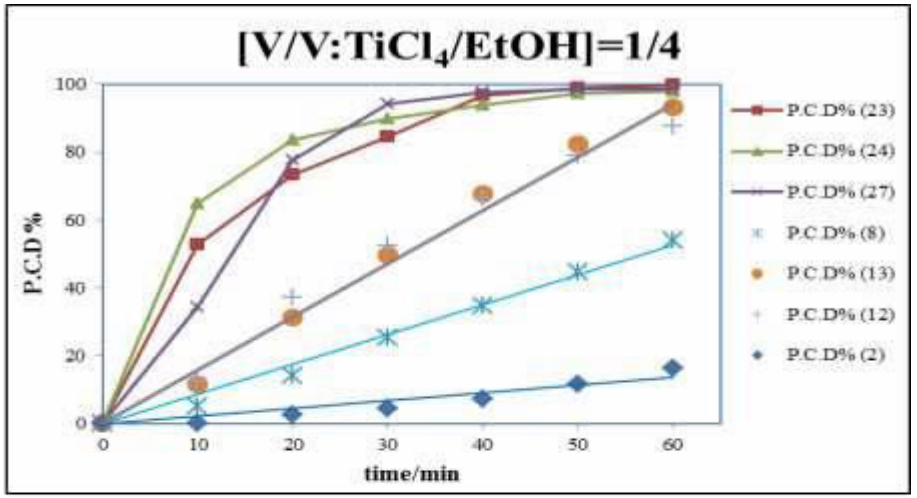

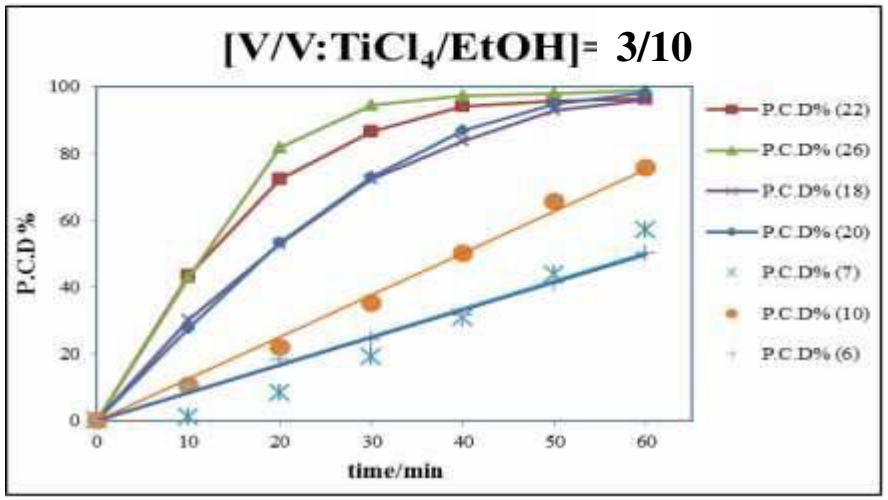

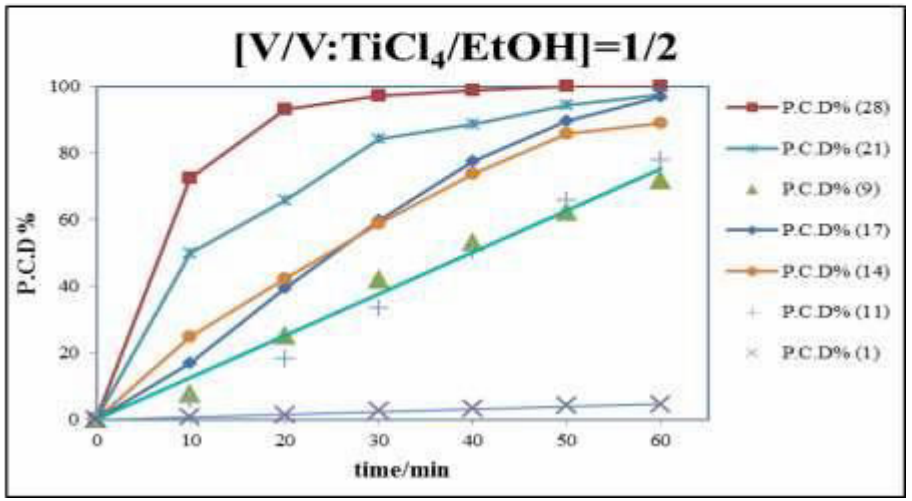

Figures 54 to 57: Photocatalytic decolorization percentage of RB 5 dye at different types of the prepared TiO_2-NPs. [V/V($TiCl_4$:EtOH)=1:10, 1:4, 1:3 and 1:2].

Variations of decolorization efficiencies

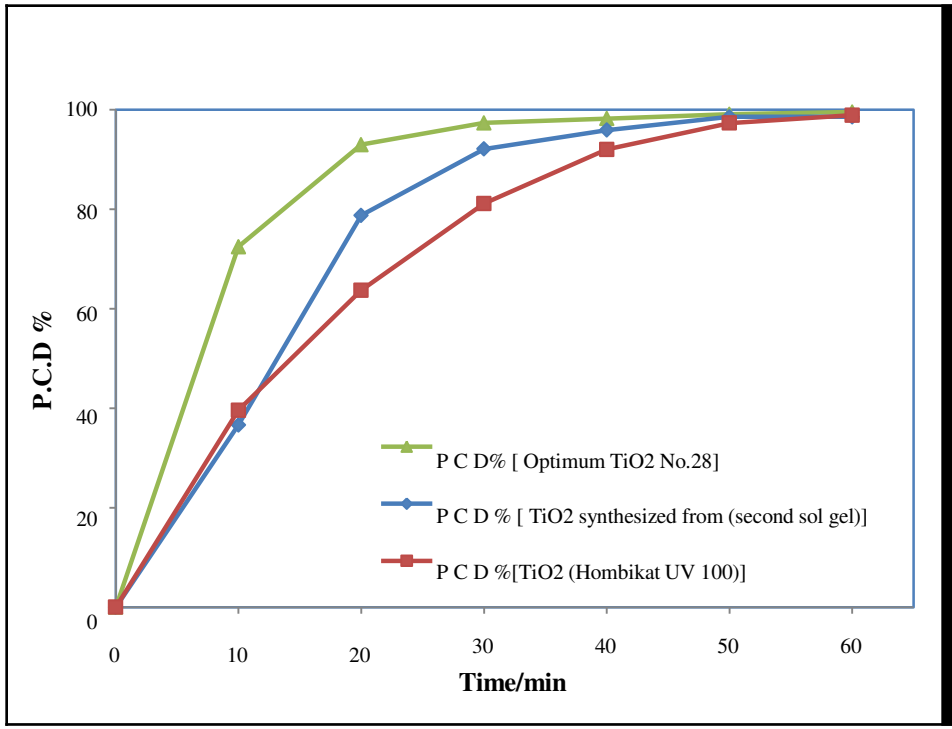

Figure 58: Photocatalytic decolorization percentage of RB 5 dye at the optimum two types of the prepared TiO_2-NPs with TiO_2 (Hombikat UV100).

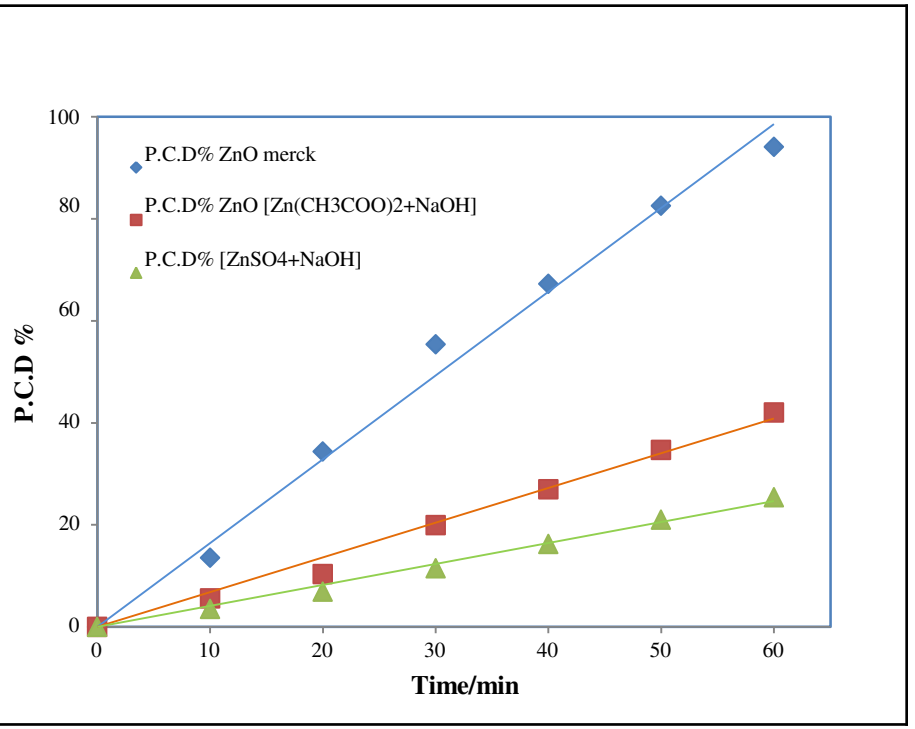

Figure 59: Photocatalytic decolorization percentage of RB 5 dye at the different two types of the prepared ZnO-NPs with ZnO (Merck).

Kinetic model of TiO_2 Nanoparticles

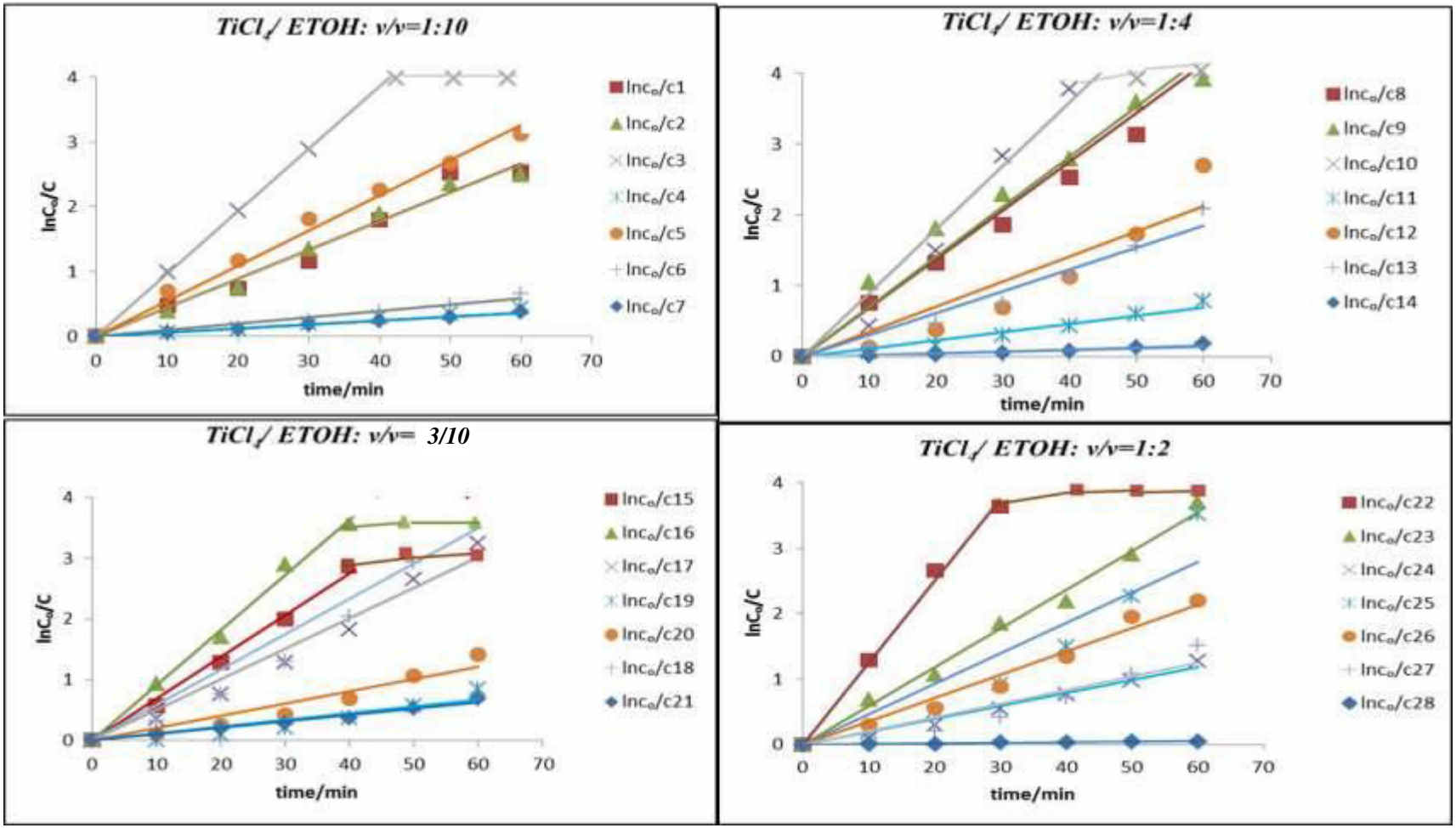

Figures 60 to 63: The change of $\ln C_o/Ct$ with irradiation time at different types of the prepared TiO_2-NPs. (V/V: $TiCl_4$/EtOH=1/10, 1:4, 1:3 and 1:2).

The TiO_2 (28) exhibited 156.625 times higher photocatalytic activity Than TiO_2 (1)

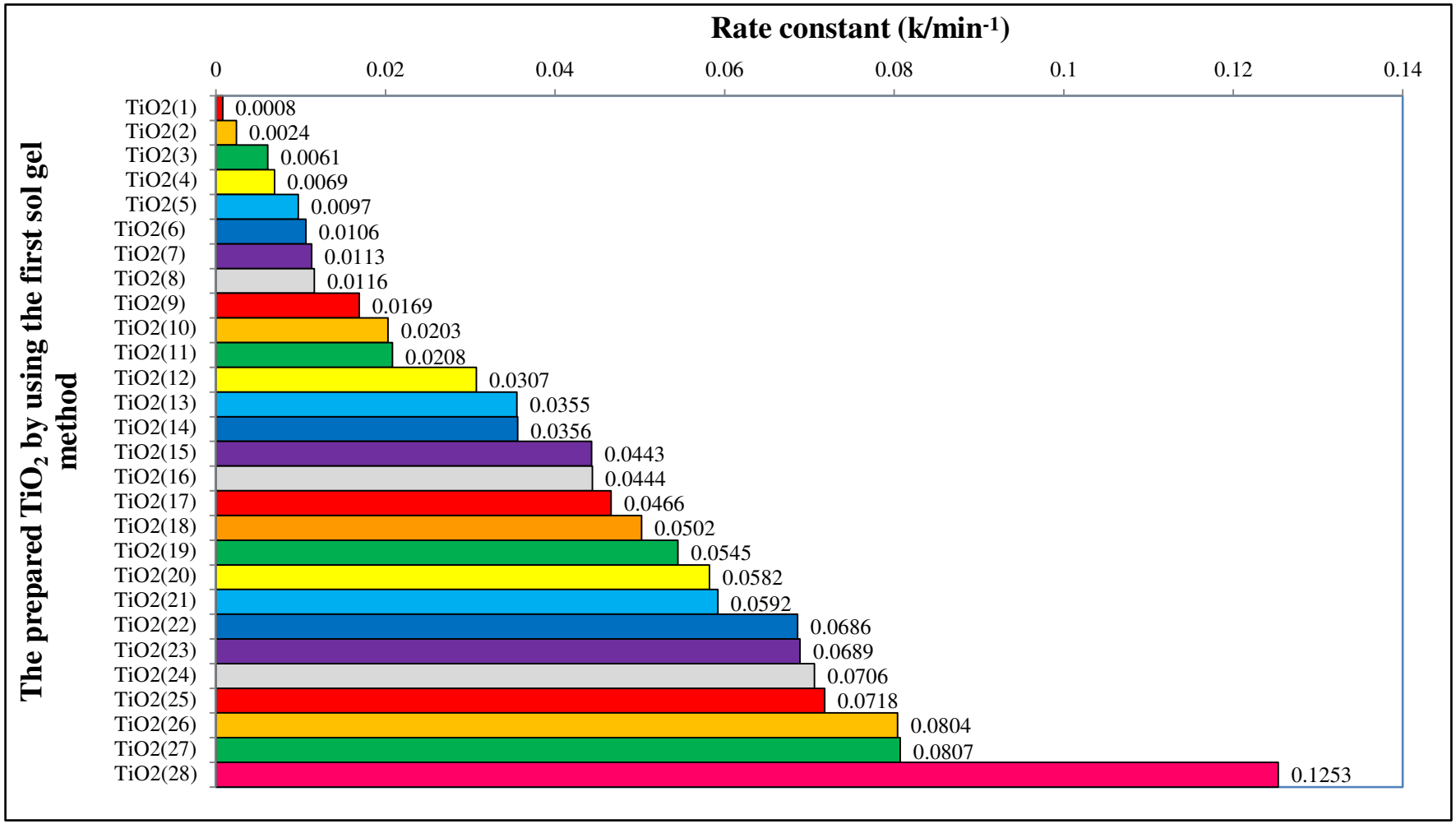

Figure 66: The variations photocatalytic activity on different types of prepared TiO_2-NPs in the first sol gel method.

The optimum prepared TiO_2-NPs by using first and second sol gel method exhibited 1.5 and 1.072 times higher photocatalytic activity Than TiO_2 (Hombikat) respectively.

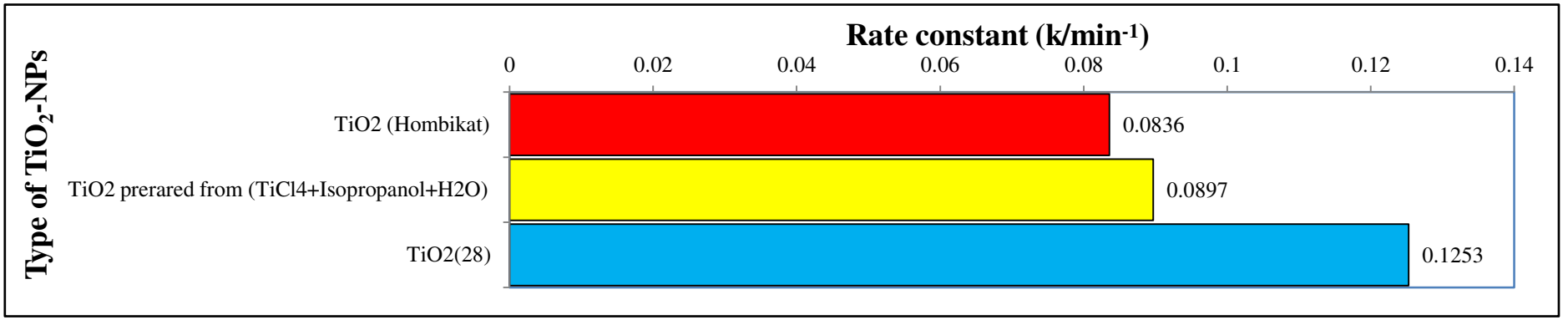

Figure 67: The comparison of photocatalytic activity on the optimum two types of the prepared TiO_2-NPs with TiO_2 (Hombikat UV100).

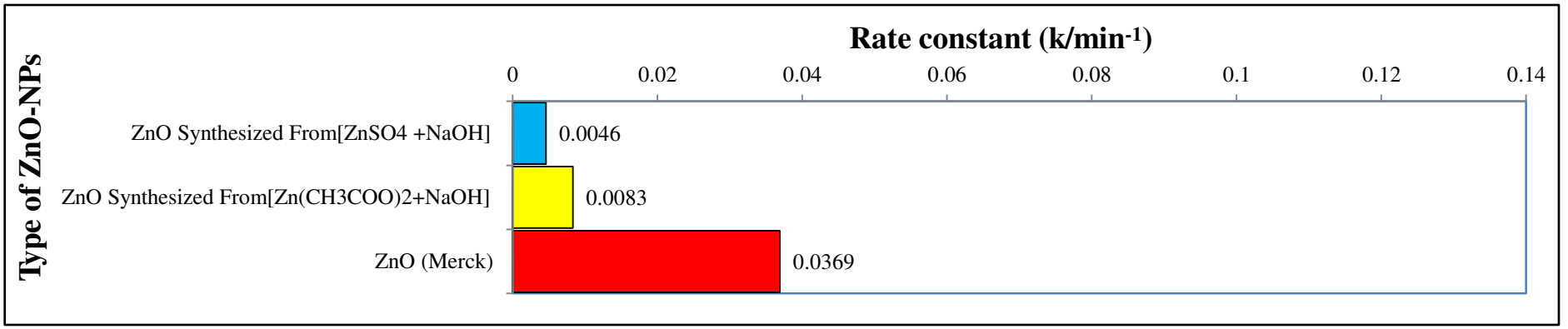

Figure 68: The comparison of photocatalytic activity on the two types of the prepared ZnO-NPs with ZnO (Merck).

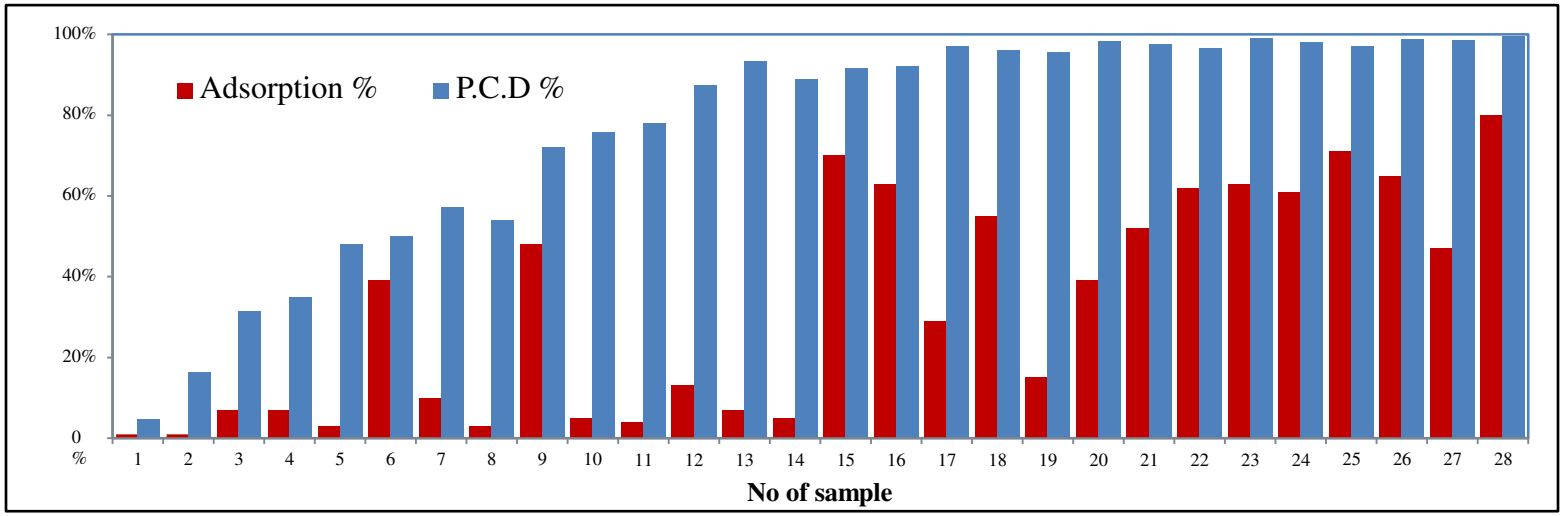

Figure 69: Comparison of Adsorption % and P.C.D % between TiO_2-NPs prepared by using first sol gel method.

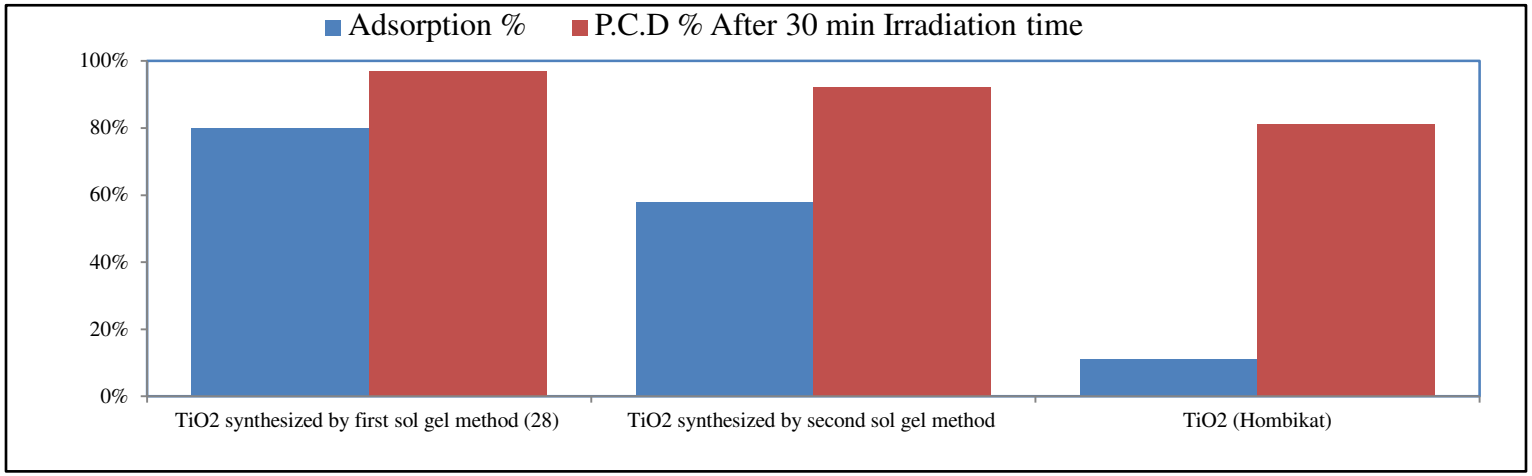

Figure 70: Comparison of Adsorption% and P.C.D% within 30 min irradiation time between optimum TiO_2-NPs prepared by using sol gel method and TiO_2 (Hombikat).

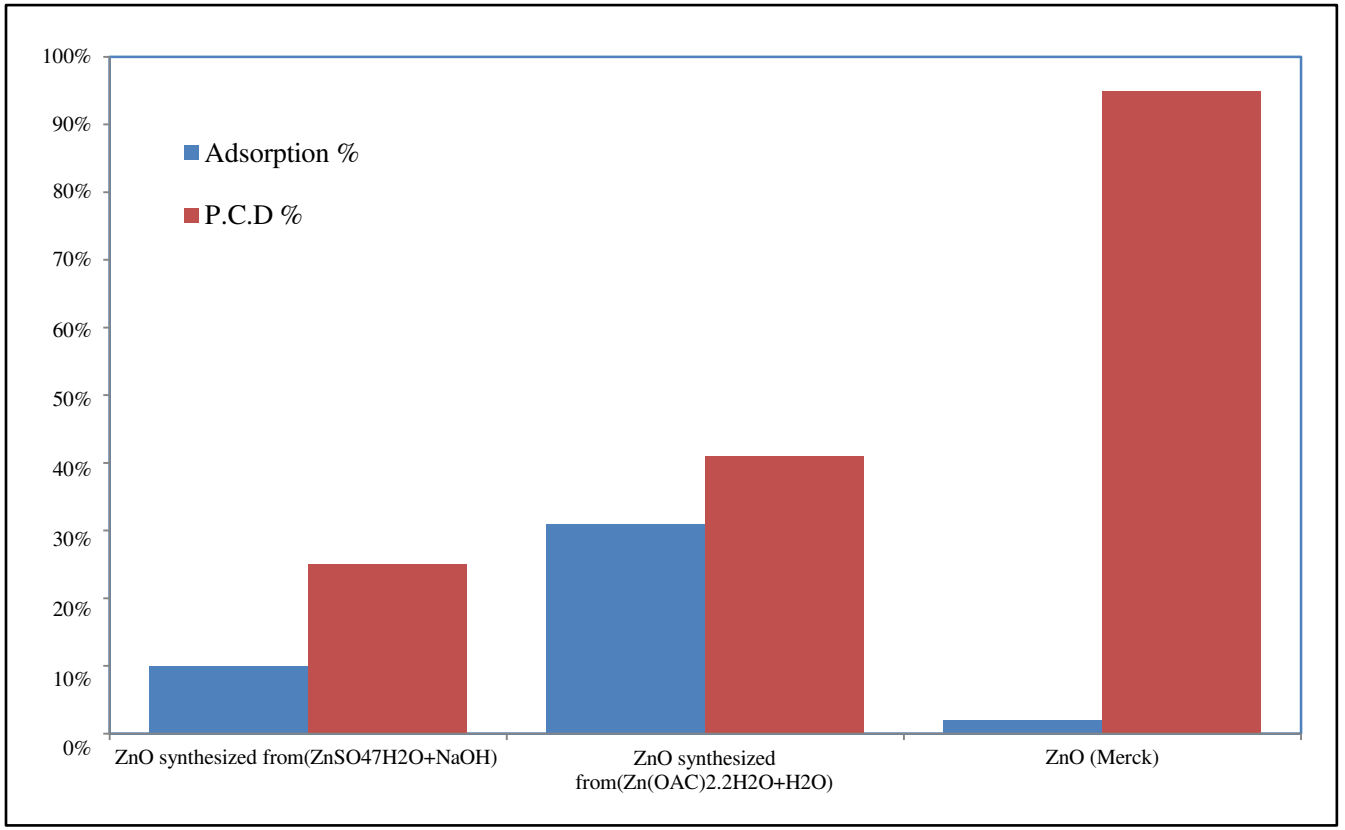

Figure 71: Comparison of Adsorption% and P.C.D% between ZnO-NPs prepared by using direct precipitation method and ZnO (Merck).

3-Combining Effect

Effect of light intensity on P.C.D of RB 5 dye in presence of optimum TiO_2-NPs

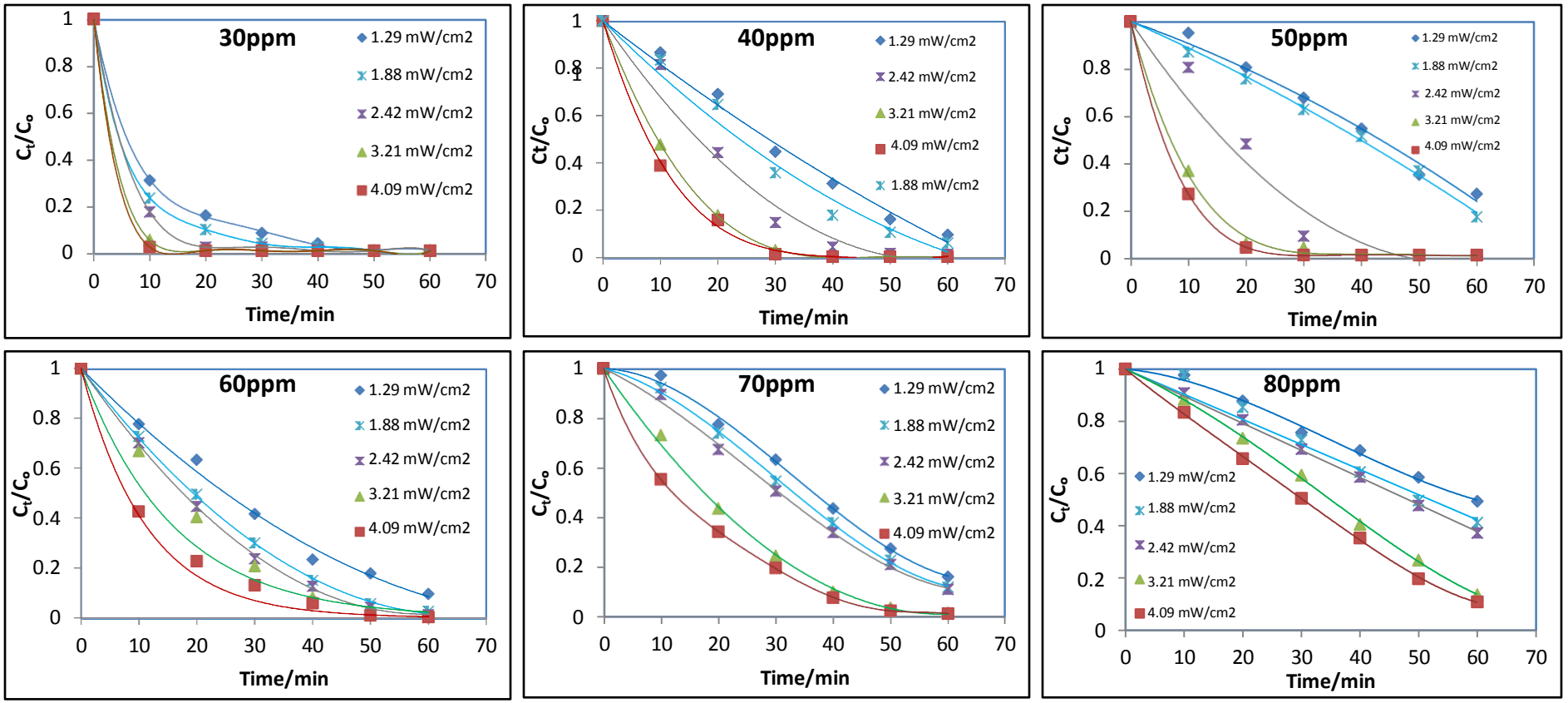

Figures 72 to 77: effect of light intensity on photocatalytic decolorization efficiency by different initial RB 5 concentration (30-80 ppm) and the optimum prepared TiO_2-NPs

Table 5: the change of rate constant with light intensity by different RB 5 concentrations.

The distance /cm	Rate constant (k / S^{-1})						Light intensity	
	30ppm	40ppm	50ppm	60ppm	70ppm	80ppm	(Einstein S^{-1})x10^{-7}	(mW/cm^2)
--	0.0000	0.0000	0.0000	0.0000	0.0000	0.0000	0.0000	0.0000
26	0.0827	0.0216	0.0392	0.0355	0.0249	0.0105	1.0726	1.2900
23	0.0915	0.0288	0.0464	0.0542	0.0292	0.0133	1.2940	1.8800
20	0.1203	0.0839	0.0726	0.0628	0.0311	0.0147	1.3940	2.4200
17	0.1355	0.1069	0.1243	0.0752	0.0622	0.0269	1.5610	3.2100
14	0.1378	0.1409	0.1340	0.0890	0.0685	0.0315	1.7592	4.0900

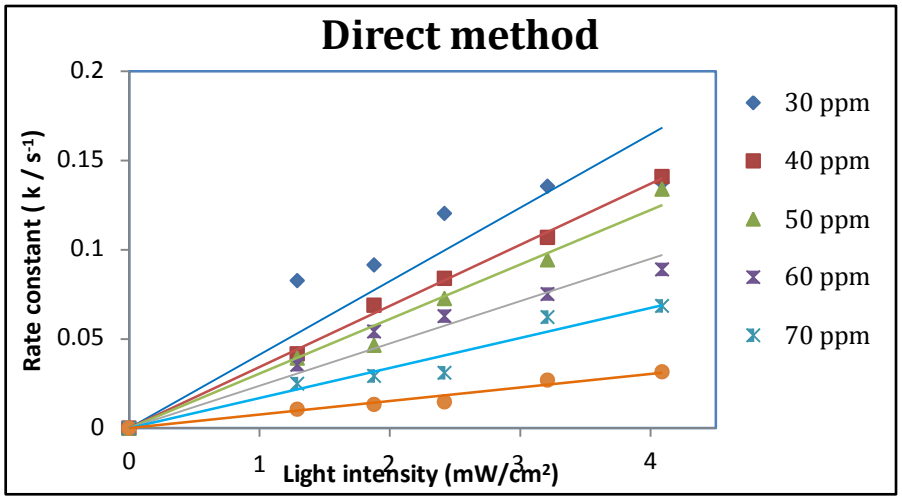

Figure 78: Effect of initial light intensity (direct method) on rate constant by different RB 5 concentration and the optimum prepared TiO_2-NPs.

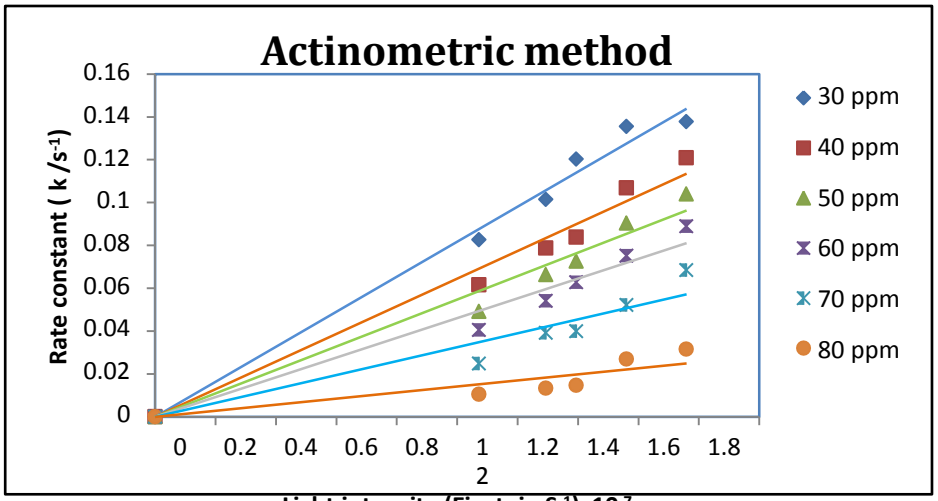

Figure 79: Effect of initial light intensity (actinometric method) on rate constant by different RB 5 concentration and the optimum prepared TiO_2-NPs.

Conclusions

1. The sol-gel method led to the formation of amorphous and crystalline TiO_2 nanomaterials by controlling the calcination temperature. It is possible to tailor the crystalline and spectroscopic properties of TiO_2-NPs.
2. A developed sol-gel technique revealed to be a good method for the preparation of TiO_2-NPs. Raising calcination temperatures led to increase in crystallite dimensions and promoted phase transformation from anatase to rutile. Pure anatase TiO_2-NPs was found to be more active than rutile or a mixtures of them, in the photocatalytic decolorization of RB 5 under UV (365 nm) light.
3. Among the prepared catalysts, the best synthesized TiO_2-NPs showed the highest adsorption (80.0%) and complete photocatalytic decolorization efficiency (100%) of RB 5. Moreover, it exhibited about 150 times higher photocatalytic activity than commercial TiO_2 (Hombikat). This catalyst has been synthesized in conditions [V/V =1:2 ($TiCl_4$:EtOH) of additives and 200°C annealing temperature].
4. Unfortunately the synthesized ZnO-NPs have lower photocatalytic activity; however, they have higher adsorption capacity than commercial ZnO (Merck).

5. On catalyst characterization, it was observed that the average crystallite size and the average particle size of all catalysts were in the range between 6.23-164.76 and 84.89-164.66 nm according to XRD and SPM, respectively. It was found that the synthesized photocatalysts exhibited smaller spherical shaped particles, amorphous with higher crystallinity and larger surface to volume ratio (S/V) and a spectacular electron transport property having a remarkable photocatalytic activity in terms of the RB 5 decomposition.
6. Adsorption results demonstrated that the prepared TiO_2-NPs was a promising adsorbent for removal of RB 5 dye from aqueous solutions.
7. The Langmuir model fitted the experimental data in the presence of optimum catalyst better than Frendlich model, indicating the adsorption tends to be monolayer adsorption.
8. The kinetic adsorption data indicated that the adsorption process in the presence of optimum catalyst was controlled by pseudo-second order equation.
9. The higher removal efficiency of RB 5 in the presence of optimum synthesized TiO_2-NPs equals to 60% at the pH 6. This behavior could be explained on the basis of zero point charge (ZPC).

10. The values of thermodynamic parameters indicate that the adsorption of RB 5 onto TiO_2-NPs was thermodynamically feasible and spontaneous.
11. The transformation from anatase to rutile occurred. Crystallites tend to agglomerate from quantum dotes to bulk size particles with the progressive loss of activity of the catalysts.
12. The photocatalytic process for all prepared catalysts can be expressed by both, the pseudo-first order reaction kinetics and the Langmuir-Hinshelwood kinetic model.
13. The phenomenon of increasing the photodecolorization efficiency of RB 5 with decreasing the concentration of solution is due to the decrease in the concentration OH^- adsorbed on catalyst surface.
14. The controlled experimental photocatalytic reaction indicated that the presence of UV light, oxygen, and catalyst are essential for the effective destruction of RB 5.
15. Photocatalytic activity results concluded that the photoefficiency of the synthesized catalysts is not only related to its intrinsic properties but also to the activating nature of the substrate to be decolorized.

16. TiO_2-NPs catalysts appeared to be very promising material for the photocatalytic degradation of several organic compounds under UV light.
17. Combining effect considering a pseudo-steady state approach was used for description of the kinetics of the photocatalytic process dependence on the initial concentration of the RB 5 and light intensity. The increase in the photon flux results to the increase of number of electron-hole pair; hence, increase in the kinetic rate constant, which is attributed to an increasing concentration of $HO^{\bullet}$ radicals accelerating the oxidation of the organic molecules.
18. From an applied point of view, photocatalytic oxidation processes using the optimum TiO_2-NPs appear to be a very useful technique for the detoxification of water containing moderate organic contents, leading to mineralization of pollutants.

References:

1) Majeed A. Shaheed and Falah H. Hussein, "Adsorption of Reactive Black 5 on Synthesized Titanium Dioxide Nanoparticles: Equilibrium Isotherm and Kinetic Studies", Journal of Nanomaterials, , vol. 2014, Article ID 198561, pp. 11.
2) S. Mukherjee, F. Libisch, N. Large, O. Neumann, L. V. Brown, J. Cheng, J. B. Lassiter, E. A. Carter, P. Nordlander, and N. J. Halas, "Hot electrons Do the impossible: plasmon-induced dissociation of H_2 on Au," Journal of Nano Lett., vol. 13, pp. 240–247, 2013.
3) G. Xin, H. Pan, D. Chen, Z. Zhang, and B. Wen, "Synthesis and photocatalytic activity of N-doped TiO_2 produced in a solid phase reaction," Journal of Physics and Chemistry of Solids, vol. 74, pp. 286–290, 2013.
4) B. Choudhury and A. Choudhury, "Tailoring luminescence properties of TiO_2 nanoparticles by Mn doping," Journal of Luminescence, vol. 136, pp. 339 –346, 2013.
5) P. K. Samanta and S. Mishra, "Solution phase synthesis of ZnO nanopencils and their optical property," Journal of Materials Letters, vol. 91, pp. 338 –340, 2013.
6) W. K. Tan, K. A. Razak, Z. Lockman, G. Kawamura, H. Muto, and A. Matsuda, "Formation of highly crystallized ZnO nanostructures by hot-water treatment of etched Zn foils, Journal of Materials Letters, vol. 91, pp. 111–114, 2013.

7) W. Li and T. Zeng, "Preparation of TiO_2 anatase nanocrystals by $TiCl_4$ hydrolysis with additive H2SO4," Journal of pone, vol. 6, no. 6, pp. 6, 2011.
8) B. Choudhury, B. Borah, and A. Choudhury, "Ce–Nd codoping effect on the structural and optical properties of TiO2 nanoparticles," Journal of Materials Science and Engineering B, vol. 178, no. 4, pp. 239–247, 2013.
9) M. C. Mathpal, A. K. Tripathi, M. K. Singh, S. P. Gairola, S. N. Pandey, and A. Agarwal, "Effect of annealing temperature on Raman spectra of TiO2 nanoparticles," Journal of Chemical Physics Letters, vol. 555, pp. 182–186, 2013.
10) A. Hoseinpur, J. V. Khaki, and M. S. Marashi, "Mechanochemical synthesis of tungsten carbide nanoparticles by using WO_3/Zn/C powder mixture," Journal of Materials Research Bulletin, vol. 48, pp. 399–403, 2013.
11) Y. G. Zhu, J. W. Eaton, and C. Li, "Titanium dioxide (TiO_2) nanoparticles preferentially induce cell death in transformed cells in a Bak/Bax-independent fashion," Journal of pone, vol. 7, no. 11, e50607, 2012.
12) A. D. Paola, M. Bellardita, and L. Palmisano, "Brookite, the least known TiO_2 photocatalyst," Journal of catalysts, vol. 3, pp. 36–73, 2013.

Chemical Sciences Related Journals

- Journal of Thermodynamics & Catalysis
- Journal of Plant Biochemistry & Physiology
- Organic Chemistry: Current Research

Chemical Sciences
Related Conferences

- Medicinal Chemistry & Computer Aided Drug Designing
- 3rd International Conference on Medicinal Chemistry & Computer Aided Drug Designing

OMICS International **Open Access Membership**

OMICS International Open Access Membership enables academic and research institutions, funders and corporations to actively encourage open access in scholarly communication and the dissemination of research published by their authors.
For more details and benefits, click on the link below:
http://omicsonline.org/membership.php